



HAL
open science

Multiple melting stages and refertilization as indicators for ridge to subduction formation: The New Caledonia ophiolite

Marc Ulrich, Christian Picard, Stéphane Guillot, Catherine Chauvel,
Dominique Cluzel, Sébastien Meffre

► To cite this version:

Marc Ulrich, Christian Picard, Stéphane Guillot, Catherine Chauvel, Dominique Cluzel, et al.. Multiple melting stages and refertilization as indicators for ridge to subduction formation: The New Caledonia ophiolite. *Lithos*, 2010, 115, pp.223-236. 10.1016/J.LITHOS.2009.12.011 . insu-00549832

HAL Id: insu-00549832

<https://insu.hal.science/insu-00549832>

Submitted on 20 Jan 2011

HAL is a multi-disciplinary open access archive for the deposit and dissemination of scientific research documents, whether they are published or not. The documents may come from teaching and research institutions in France or abroad, or from public or private research centers.

L'archive ouverte pluridisciplinaire **HAL**, est destinée au dépôt et à la diffusion de documents scientifiques de niveau recherche, publiés ou non, émanant des établissements d'enseignement et de recherche français ou étrangers, des laboratoires publics ou privés.

Multiple melting stages and refertilization as indicators for ridge to subduction formation: The New Caledonia ophiolite

Marc Ulrich^{a, b, *}, Christian Picard^c, Stéphane Guillot^b, Catherine Chauvel^b, Dominique Cluzel^a and Sébastien Meffre^d

^a PPME, EA 3325, Université de la Nouvelle-Calédonie, 98851, Nouméa, Nouvelle-Calédonie

^b LGCA-CNRS, UMR 5025, Université Grenoble 1, 38041, Grenoble, France

^c UMR 6249 Chrono-environnement, Université de Franche Comté, 25000, Besançon, France

^d ARC Centre of Excellence in Ore Deposits, University of Tasmania, Australia

Abstract

The origin of the New Caledonia ophiolite (South West Pacific), one of the largest in the world, is controversial. This nappe of ultramafic rocks (300 km long, 50 km wide and 2 km thick) is thrust upon a smaller nappe (Poya terrane) composed of basalts from mid-ocean ridges (MORB), back arc basins (BABB) and ocean islands (OIB). This nappe was tectonically accreted from the subducting plate prior and during the obduction of the ultramafic nappe.

The bulk of the ophiolite is composed of highly depleted harzburgites (\pm dunites) with characteristic U-shaped bulk-rock rare-earth element (REE) patterns that are attributed to their formation in a forearc environment. In contrast, the origin of spoon-shaped REE patterns of lherzolites in the northernmost klippen was unclear. Our new major element and REE data on whole rocks, spinel and clinopyroxene establish the abyssal affinity of these lherzolites. Significant LREE enrichment in the lherzolites is best explained by partial melting in a spreading ridge, followed by near in-situ refertilization from deeper mantle melts. Using equilibrium melting equations, we show that melts extracted from these lherzolites are compositionally similar to the MORB of the Poya terrane. This is used to infer that the ultramafic nappe and the mafic Poya terrane represent oceanic lithosphere of a single marginal basin that formed during the late Cretaceous. In contrast, our spinel data highlights the strong forearc affinities of the most depleted harzburgites whose compositions are best modeled by hydrous melting of a source that had previously experienced depletion in a spreading ridge. The New Caledonian boninites probably formed during this second stage of partial melting.

The two melting events in the New Caledonia ophiolite record the rapid transition from oceanic accretion to convergence in the South Loyalty Basin during the Late Paleocene, with initiation of a new subduction zone at or near the ridge axis.

Keywords: New Caledonia; Ophiolite; Refertilization; Peridotite; Partial melting; Rare earth element

1. Introduction

It is now clearly established that ophiolites represent segments of obducted oceanic lithosphere. In that sense, they provide a unique opportunity to study the physical and chemical processes that affect the upper mantle in mid oceanic and subduction environments. The Cretaceous to Eocene New Caledonia ophiolite is an extensive and very well-exposed mafic–ultramafic complex ([Avias, 1967], [Collot et al., 1987] and [Prinzhofer, 1981]) that is still partially connected to the modern oceanic floor of the South Loyalty Basin to the east of the island (Fig. 1). The ophiolite is dominated by harzburgites and dunites; minor spinel and plagioclase lherzolites are restricted to the northernmost massifs.

Considerable discussion has focused on the origin and tectonic setting of the ultramafic rocks. Lherzolitic massifs worldwide have characteristics consistent with generation from a depleted mantle that had been affected by secondary magmatic impregnation ([Nicolas and Dupuy, 1984], [Takazawa et al., 2003], [Muntener et al., 2004], [Niu, 2004], [Le Roux et al., 2007], [Piccardo et al., 2007] and [Barth et al., 2008]). Many lherzolites are thought to form in fertile mid-oceanic environments ([Boudier and Nicolas, 1985] and [Nicolas and Boudier, 2003]) but previous studies of the New Caledonia peridotites suggest that they come from a supra-subduction setting ([Cluzel et al., 2001], [Whattam, 2008] and [Whattam et al., 2008]). Similarly, the close spatial and temporal association in the magmatic Poya terrane of New Caledonia of MORB ([Eissen et al., 1998] and [Cluzel et al., 2001]) and boninites ([Sameshima et al., 1983] and [Cameron, 1989]) provides evidence for magmatism in mid-ocean ridge and forearc subduction settings ([Whattam, 2008] and [Whattam et al., 2008]).

The aim of this study is to determine the origin of the ophiolite and the nature of the petrological processes resulting in the diversity of the peridotites. Using major and rare earth element analyses, we modeled the geochemical trends of residual peridotites from both ridge and supra-subduction zone environments and compared the results with the New Caledonia peridotites. We finally discuss the association of the peridotites with the genesis of MOR-type melts of the underlying Poya terrane. Our results suggest that the lherzolites and harzburgites of the New Caledonia ophiolite record two stages of partial melting in the South Loyalty Basin as it evolved from an ocean ridge to a subduction setting.

2. Geological setting and petrologic description

New Caledonia lies on the Norfolk ridge, 2000 km east of Australia (Fig. 1). Both the ridge and the island form part of a tectonic patchwork of Permian to Eocene volcano-sedimentary terranes that were amalgamated during two periods of convergence, the first in the Early Cretaceous (Rangitata orogen) (Paris, 1981) and the second in the Late Eocene (Alpine orogen) ([Paris, 1981] and [Aitchison et al., 1995]). The two periods were separated by the opening of marginal basins such as the Late-Cretaceous to Paleocene Tasman Sea and the New Caledonian and South Loyalty Basins. Allochthonous Cretaceous to Paleocene ophiolites now overlie Carboniferous–Eocene basement of the island of New Caledonia.

The Poya volcanic terrane is exposed on both sides of the northern part of the island. It is overlaid by three small ultramafic bodies, the Koniambo Massif, the Tiebaghi Massif and the Poum Massif and the much larger Massif du Sud that forms most of the southern part of the island (Fig. 2). These massifs are the focus of our study.

2.1. The magmatic Poya terrane

The Poya terrane is mainly exposed between Noumea and Koumac on the west coast of New Caledonia, as well as beneath the peridotites on the east coast (Poindimié and Touho sectors) (Fig. 2). The Poya terrane is interpreted as a set of tectonic slices of oceanic crust that were scraped off the down-going plate (the South Loyalty Basin), in front of the Loyalty arc, and then thrust “en bloc” onto the Norfolk Ridge basement during the Late Eocene (Cluzel et al., 2001).

Although some previous studies (e.g. Paris, 1981) argued that Poya terrane is autochthonous, an allochthonous origin, based upon tectonic, geochemical and stratigraphic evidence ([Aitchison et al., 1995], [Cluzel et al., 1997], [Cluzel et al., 2001] and [Eissen et al., 1998]), is now widely accepted. Likewise, considering the chemical composition of both terranes, it is now clearly established that the Poya terrane cannot be considered as the detached cover of the overlying ultramafic terrane (Eissen et al., 1998).

(Cluzel et al., 1994), (Cluzel et al., 1997), (Cluzel et al., 2001), (Aitchison et al., 1995) and (Eissen et al., 1998) have described the petrological, mineralogical, geochemical and micropaleontological aspects of the terrane, which may be summarized as follows. The Poya terrane is mainly composed of pillow basalts and dolerites with minor abyssal argillites that contain Campanian to Late Paleocene or Early Eocene radiolarians. MORB-type tholeiites dominate (ca. 90%) but minor back-arc basin basalts (BABB, ca. 5%), and ocean island basalts (OIB) are also present ([Eissen et al., 1998] and [Cluzel et al., 2001]). Calcareous sediments containing Early- to Mid-Eocene foraminifera are interlayered with the back-arc and ocean island basalts (D. Cluzel, unpublished data), which probably represent small seamounts on older (Campanian–Early Eocene) MORB crust.

Boninites are found in rare, small outcrops close to the serpentized peridotite thrust sheets near Koné (Fig. 2). These black and extremely well-preserved glassy rocks occur as dykes or pillow lavas. Although these boninites appear to form part of the Poya terrane, isotopic data published by Cameron et al. (2003) demonstrate that these rocks are petrogenetically and tectonically unrelated to the magmatic terrane.

2.2. The New Caledonian Ultramafic Nappe

Ultramafic rocks, mainly harzburgites and minor dunites, outcrop extensively throughout New Caledonia. The largest continuous massif (the Massif du Sud) occurs in the south of the island. Smaller isolated klippe along the west coast of the main island (La Grande Terre) are connected to submarine outcrops that extend approximately 300 km north of the island (Collot and Missègue, 1988). The ultramafic rocks are thought to be oceanic lithosphere of the Loyalty Basin that was obducted at the end of the Late Eocene when the Loyalty arc collided with the Norfolk continental ridge ([Collot et al., 1986], [Aitchison et al., 1995] and [Cluzel et al., 2001]).

2.2.1. The Massif du Sud

The Massif du Sud covers an area of approximately 6000 km² (Fig. 2). It is characterized by harzburgites with local intercalations of chromite-rich dunites and orthopyroxenites that are overlain by a lower crustal cumulate sequence containing dunite, wehrlite, pyroxenite and

gabbro (Fig. 3) The cumulate rocks are restricted to the southern and the upper part of the massif (Prinzhofer, 1981).

The harzburgite from the mantle sequence consists of olivine (80 to 90%, locally serpentinized), orthopyroxene (10 to 20%) and minor spinel (<1%). Clinopyroxene is only found in pyroxenite dykes. On the eastern side of the Massif du Sud (Poro sector, Fig. 2), exceptionally fresh and well-preserved peridotites have primary mineralogical compositions identical to the more serpentinized rocks of the rest of the massif.

Cumulates from the Montagne des Sources (Fig. 2) area, consist of alternating dunites and gabbros at three superposed levels. At the bottom, ribbon-shaped, 1–10 m-thick folded layers of dunite rest directly on mantle harzburgites. The middle level is composed by various rock types — wehrlite, orthopyroxenite, clinopyroxenite and websterite — and the upper level is mainly composed of gabbro and gabbro-norite. As previously pointed out, mafic volcanic rocks comagmatic with the New Caledonia ophiolitic sequence are absent.

2.2.2. The Koniambo massif

The Koniambo massif, in the Koné area, is composed of three lithological assemblages that overlie the Poya terrane: a strongly serpentinized harzburgite–dunite sequence at the base, followed by a spinel dunite sequence and a succession of sheets composed of harzburgite and minor dunite (Fig. 3) (Audet, 2008).

The basal harzburgite–dunite unit is totally serpentinized and highly silicified. The overlying dunites are homogenous and fine grained. Olivine, 30% serpentinized is associated with less than 1% of orthopyroxene and spinel.

The uppermost sequence is mainly composed of harzburgite and sheets of dunite. The proportion of orthopyroxene increases from the bottom to the top of the sequence. Clinopyroxene is locally present as an accessory phase in the upper part of the massif and rare dunite forms thin (<1 m) and discontinuous horizons.

2.2.3. The Tiebaghi massif and the Poum massif

These massifs occur at the far northwestern coast of the island. According to (Moutte, 1979) and (Sécher, 1981) the massifs are composed of pyroxene-rich mantle peridotite associated with pyroxenite and chromitite with no overlying crustal sequence (Fig. 3). The degree of serpentinization decreases from near 100% in the lower serpentinized and silicified layer to about 60% in the upper part of the massif. The proportion of pyroxene, first orthopyroxene and then clinopyroxene, also increases from the base to the top.

Harzburgite is the dominant lithology in the Tiebaghi massif, while the Poum massif is composed mainly of spinel and plagioclase lherzolites. The composition of the harzburgites is variable: the orthopyroxene content varies from 10 to 50% of the rock and coexists with minor spinel (1%) and diopside (up to 1%). This sequence alternates with ≤ 40 m thick dunite layers.

Spinel and plagioclase lherzolites from the upper units of the massifs exhibit porphyroblastic textures characterized by large orthopyroxene grains (5–12 mm) with diopside exsolution lamellae and moderately serpentinized olivine grains. Millimeter-sized spinel grains are

associated with the orthopyroxene porphyroblasts. Clinopyroxene comprises 5–10% of the spinel lherzolites, and up to 15% of plagioclase lherzolites. It is sometimes interstitial, with lobate rims (Fig. 4), and is either associated with orthopyroxene and spinel or altered plagioclase. Plagioclase also displays rounded shapes and is typically interstitial between olivine grains (Fig. 4). It sometimes forms coronas around small rounded grains of pyroxene, olivine or spinel.

3. Geochemical data

Whole rock major and rare earth element (REE) analyses of samples from the Massif du Sud, the Koniambo, the Tiebaghi and the Poum massifs were performed at the LGCA (University of Grenoble, France) (Table 1).

Concentrations of major elements were determined by ICP-AES using a Perkin Elmer 3000 DV spectrometer using the method of [Cotten et al. \(1995\)](#). Our results agree well with reference values of [Govindaraju \(1995\)](#) for the serpentinite standard UB-N. Analytical uncertainties are <2% for SiO₂ and <5% for other major elements (except for K₂O and P₂O₅, which are present in very low concentrations).

REE concentrations were determined by a method derived from [Barrat et al. \(1996\)](#) using an Agilent 7500ce ICP-MS. About 100 mg of powder were dissolved in a HF-HClO₄ mixture (5:1) in Teflon containers. Complete dissolution was achieved in steel jacketed PARR bombs for 5 days at 140 °C. REE were purified using AG50W-X8 200-400 mesh cation-resin ion-exchange columns. The international standard BHVO-2 was used to calibrate the ICP-MS, and the UB-N serpentinite standard was analyzed as an unknown. Measured blanks for each REE taken separately were generally much lower than 10 pg and are thus negligible in comparison with the total amount of REE processed during sample analysis. The precision obtained by our method is indicated by the relative standard deviation (RSD) values, based on multiple determinations made in independent analytical procedures. The RSD values for all REE are <5%, and results on UB-N are consistent with the values previously published by [Garbe-Schonberg \(1993\)](#).

The major element compositions of spinels ([Table 2](#)) were obtained using Central Science Laboratory Cameca SX100 electron microprobe on thin sections at the University of Tasmania using pure metals and mineral standards.

Clinopyroxene crystals from 4 different samples ([Table 3](#)) were separated to analyze their REE contents. Samples were crushed and sieved to retain the 160 to 200 µm fractions then clinopyroxene was separated using Frantz magnetic separator prior to hand picking and mounting into a 2.5 mm epoxy mount. The REE compositions were determined using an Agilent 7500cs ICPMS and a New Wave 193 nm solid state laser at the University of Tasmania. Ablation was performed using a 100 micron spot size with the laser pulsing at 10 Hz in a custom-made chamber in an He atmosphere. Concentrations were determined using the standard glass NIST 612 analyzed about every hour using ⁴³Ca (determined from the electron microprobe) as the internal standard element. A secondary standard glass (BCR-2) was also analyzed at the same time as the samples. Measured values for the standard BCR-2 are similar to those published by [Jochum and Nohl \(2008\)](#).

3.1. Major elements

Major element concentrations are typical of serpentinized peridotite (loss on ignition ~ 10 wt.%). Samples from the northern massifs record large compositional range with wide variation in the Al₂O₃ and MgO contents and considerable scatter of CaO and SiO₂ (Fig. 5C,D). Except for CaO, correlation trends observed for the lherzolites between element oxides and MgO abundance are consistent with those defined for abyssal peridotites (Niu et al., 1997). In contrast, harzburgites in all the massifs are more homogeneous with lower Al₂O₃, Na₂O and K₂O and higher MgO contents.

Compared to modern peridotites from well-constrained tectonic settings ([Ishii et al., 1992], [Niu, 2004] and [Hattori and Guillot, 2007]), the lherzolites from northern massifs in New Caledonia are similar in composition to abyssal peridotite while harzburgites from the entire ophiolite are similar to typical Mariana forearc peridotites (Fig. 5).

3.2. Whole rock rare earth elements

The whole rock REE contents in all samples is low, < 10⁻² ppm. Each lithology has a distinctive pattern (Fig. 6): harzburgites from all massifs are characterized by marked enrichments of the LREE and HREE over the MREE (U-shaped patterns), and peridotites from northern massifs (Tiebaghi and Poum) are slightly less depleted in M- and HREE than those from the centre (Koniambo) and south (Massif du Sud) of the island. Prinzhofer and Allegre (1985) reported systematic negative Eu anomalies, but our samples display both negative and positive Eu anomalies (Eu/Eu* = 0.33–6.78). The REE contents of lherzolites from the northern massifs are different to those of the harzburgites. The lherzolites show strong LREE depletion with a slight enrichment in La–Ce–Pr and the plagioclase lherzolites are systematically more REE-enriched than the spinel lherzolites.

3.3. Spinel

Spinel in plagioclase-free peridotite of the northern massif (Fig. 7) is relatively magnesian-rich (Mg# >0.6) with low chromian content (Cr# ≈ 0.3) and plots in the field of abyssal peridotites. In contrast, spinel from the Massif du Sud and the Koniambo massif has lower Mg# (0.4 to 0.6) and higher Cr# (0.55 to 0.75). Spinel from plagioclase lherzolites has compositions intermediate between the most fertile and the most refractory peridotites. Ti contents are significantly higher (> 0.25%) than the other peridotite spinel (<0.1%).

3.4. Rare earth elements in clinopyroxene

All clinopyroxenes analyzed in this study have steeply plunging LREE patterns with flat to humped M- to HREE pattern (Fig. 8). They are similar to abyssal peridotites ([Johnson et al., 1990] and [Johnson and Dick, 1992]) but different from supra-subduction peridotites (Parkinson et al., 1992). Clinopyroxene from plagioclase lherzolites (Ti 48.06, Poum 11 and Poum 13; Table 3) display negative Eu anomalies (Eu/Eu* = 0.46 to 0.75) that result from equilibration with the plagioclase. Clinopyroxene from the sample Poum 11 has lower REE contents than in other samples which suggests a higher degree of partial melting.

4. Discussion

Our new geochemical data show that the differences between peridotites from the Massif du Sud and the northern massifs are probably due to various degrees of partial melting. However, special features such as LREE enrichment marked by U-shaped patterns require an additional process.

The discussion below begins with the possible relationships between origin of the New Caledonia ophiolite, the degree of partial melting, and the processes responsible for the LREE enrichment and U-shaped REE patterns. We then use these results to shed some light on the geodynamic settings in which the rocks formed.

4.1. Effects of serpentinization

First we evaluate the influence of serpentinization on the chemical element budgets of the peridotites. The effects of the serpentinization on element mobility are now well documented (e.g. [Niu, 2004], [Iyer et al., 2008] and [Deschamps et al., 2010]). For example, it is now clearly established that the high field strength elements (HFSE) are largely immobile both during hydration on the seafloor (Niu, 2004) and during serpentinization of forearc mantle (You et al. 1996). Niu (2004) showed that major elements are generally immobile if the serpentinization only affects the olivine, in which case only MgO is generally slightly depleted. However, when clinopyroxene is altered, CaO is removed. This observation explains why CaO concentrations in the lherzolites are so scattered in Fig. 5.

The origin of the LREE enrichment is unclear. Although some studies suggest that LREE are enriched during the hydration of the peridotites (Niu, 2004), most studies have concluded that LREE enrichment in serpentinized abyssal peridotites is related to post-melting refertilization rather than hydrothermal alteration ([Navon and Stolper, 1987], [Bodinier et al., 1990], [Takazawa et al., 1992], [Takazawa et al., 2003], [Niu, 2004] and [Li and Lee, 2006]). Deschamps et al. (2010) showed that the REE remain immobile during serpentinization of abyssal and forearc peridotites. Finally, the crystallization of interstitial plagioclase in our lherzolites also indicates a secondary melt impregnation since several studies (e.g. [Muntener et al., 2004] and [Piccardo et al., 2007]) show that plagioclase in ultramafic rocks derives from the crystallization of ascending melts.

4.2. Origin of the protoliths

Eissen et al. (1998), Crawford et al. (2003), Whattam (2008) and Whattam et al. (2008) suggested that the New Caledonia ophiolite is a supra-subduction forearc mantle nappe. Our results are in partial agreement with this hypothesis.

Refractory peridotites (harzburgites) from all the massifs display evidence of supra-subduction processes; these peridotites are highly depleted and have geochemical characteristics compatible with a forearc environment (Fig. 5 and Fig. 7). An origin in highly refractory mantle is strongly supported by the high Cr in spinels (Fig. 7) which is generally thought to indicate hydrous melting in forearc settings ([Dick and Bullen, 1984] and [Ahmed et al., 2005]). The hydrous melting hypothesis is bolstered by the positive Eu anomalies, which are also observed in peridotites from the Othris ophiolites and are explained by hydrous melting in the presence of Eu-enriched fluids (Barth et al., 2008).

The presence of lherzolite in the northern massifs is more difficult to explain, because the degree of partial melting required to generate a lherzolite residue is much lower than that in

the mantle wedge. Numerous studies of lherzolite massifs around the world have cited the lherzolites from New Caledonia as an example of the refertilization that results when mantle melts infiltrate refractory harzburgite ([Takazawa et al., 1992], [Takazawa et al., 2003], [Muntener et al., 2004], [Le Roux et al., 2007], [Piccardo et al., 2007] and [Barth et al., 2008]). Partly on this basis it has been suggested that the majority of lherzolitic massifs actually represent re-fertilized rather than pristine mantle (Le Roux et al., 2007). Nicolas and Dupuy (1984) concluded that the lherzolites from New Caledonia represent refractory upper mantle impregnated by liquid resulting from partial melting of a depleted source. Our samples show only rare mineralogical evidence for re-enrichment in the form of lobate outlines of clinopyroxene grains and the occurrence of interstitial plagioclase. Nevertheless, the slight enrichment in LREE relative to MREE that we observed in bulk rocks is inconsistent with a simple melt extraction process and suggests additional processes such as post-melting reaction between residual peridotite and LREE-enriched melt ([Navon and Stolper, 1987], [Bodinier et al., 1990], [Takazawa et al., 1992], [Takazawa et al., 2003], [Niu, 2004] and [Li and Lee, 2006]).

4.3. Evaluation of partial melting degrees

4.3.1. Results from major elements

Major elements can be used to estimate the variations in the degree of partial melting ([Niu, 1997], [Takazawa et al., 2000], [Takazawa et al., 2003] and [Barth et al., 2008]), because whole rock compositions are not affected by melt percolation if the melt/peridotite ratio is low (Takazawa et al., 1992). Compositional trends were calculated using the empirical model of Niu (1997), with pressure range of 2.5–0.4 GPa. The trends for polybaric near-fractional melting gave the best fit to the sample trends, particularly at the highest degrees of partial melting (Fig. 5). An isobaric batch-melting model was also applied and gave similar results (not shown here).

Except for CaO, all calculated trends fit reasonably well with element abundances. The polybaric near-fractional melting model defines a large range in Al₂O₃–MgO space (Fig. 5A), consistent with degrees of partial melting from about 5 to 20% for the northern massif samples, with a main group centered on 15%. Harzburgites from all massifs have high MgO contents, with very low CaO and Al₂O₃ which imply high degrees of partial melting (20–27%) (Fig. 5A,C). Moreover, the position of the harzburgites to the right of the melting trend can be explained by melting in hydrous conditions, since hydrous melting produces residua with higher MgO contents at a given partial melting degree (Barth et al., 2008). This interpretation is also consistent with Cr content of spinel, since Cr# is higher than 0.55, which suggests high degrees of melting, probably under hydrous conditions, for all studied harzburgites.

Results obtained with the isobaric batch-melting model are essentially the same for the lherzolites, but suggest slightly higher degrees of partial melting for the most depleted samples. Furthermore, the FeO and SiO₂ contents of the residue are poorly constrained at a given MgO, using constant pressure. Sample trends are better constrained if pressure is allowed to vary from 2.5 to 0.4 GPa. As mentioned in section 1 of the discussion and illustrated in the CaO–MgO diagram (Fig. 5C), some of the Tiebaghi massif data plot away from the calculated trends. We attribute this Ca loss to hydrothermal alteration, a process which is confirmed by the width of the abyssal peridotite field that emphasizes the great variability of CaO in these rocks. Likewise, in the SiO₂–MgO diagram (Fig. 5D), all samples

have slightly higher SiO₂ concentrations than those expected from polybaric near-fractional melting. Although late silica enrichment is observed in the basal serpentinite layer of the New Caledonia ophiolite, it is uncommon in the upper layers. Furthermore, such SiO₂ enrichment is also observed in environments where no silica-rich fluid has circulated ([Takazawa et al., 2000], [Takazawa et al., 2003], [Niu, 2004] and [Barth et al., 2008]). Niu (2004) suggested that the high SiO₂ values are an artifact resulting from the slight MgO depletion commonly observed during serpentinization and amplification of the SiO₂ content by normalization of the data to 100 wt.% on an anhydrous basis.

4.3.2. Constraints from heavy rare earth elements

Melting trends computed with an incremental non-modal batch-melting model (dry melting) and fractional melting (Shaw, 1970) give very similar results, as shown in Fig. 9. The influence of fluid addition on the residue composition was calculated using the hydrous melting model of Bizimis et al. (2000). Parameters used in both models are shown in Table 4. The calculated partial melting degrees based on the REE are 13 to 20% for the peridotites from the Tiebaghi massif, 15% to 22% for the Poum massif (25% for one sample), and 20 to > 25% for both Massif du Sud and Koniambo massif. These results are in good agreement with the results from major elements. Moreover, the hydrous melting trend better fit the bulk of the most depleted samples. This is consistent with previous observations from major elements (i.e. CaO vs MgO diagram) and spinel data, suggesting that the highly depleted samples were produced by a hydrous melting process, probably in a supra-subduction environment.

4.4. LREE re-enrichment and link with the Poya terrane

4.4.1. Lherzolite refertilization

To model the refertilization we used an incremental, non-modal batch-melting model (Shaw, 1970). The starting material consists of a spinel lherzolite with 58% olivine, 19% orthopyroxene, 18% clinopyroxene and 5% spinel. The REE contents were those of McDonough and Sun's (1995) pyrolite. Other parameters are in Table 4 and the results are presented in Fig. 10. The calculated melt has a flat MORB-type REE pattern similar to those of the undepleted MORB of the Poya terrane. The resulting residue reproduces the HREE and MREE trend of the lherzolites, but is strongly depleted in LREE whereas our lherzolites show slight enrichment in La and Ce (Fig. 10A). The measured patterns can be modeled by the mantle–melt interaction process proposed by Kelemen et al., 1990 P.B. Kelemen, K.T.M. Johnson, R.J. Kinzler and A.J. Irving, High-field-strength element depletions in arc basalts due to mantle–magma interaction, *Nature* **345** (6275) (1990), pp. 521–524. Kelemen et al. (1990); i.e. migration of 0.01 to 0.1% of LREE-enriched melts through a peridotite that had experienced prior MORB extraction (Fig. 10A).

The melting of a more depleted mantle source forms melts similar to the back arc basin basalts (BABB) of the Poya terrane (Fig. 10B) and the calculated REE contents of the residue are similar to those of the peridotites.

The small amount of melt needed to reproduce the LREE enrichment of the lherzolites has no influence on abundance of major elements and incompatible elements such as Ti and the HREE ([Niu, 2004] and [Barth et al., 2008]). Such small amount of melt can also account for the scarcity of mineralogical and textural evidence for refertilization. For comparison, the

lherzolites from the northern Fizh block in Oman, in which textural evidence for refertilization is obvious, require the addition of 4 to 8% of MORB-type melts to account for their REE composition (Takazawa et al., 2003).

This is also confirmed by clinopyroxene chemistry. Indeed, clinopyroxene composition is important to discriminate between rock forming processes, and there are meaningful differences in composition between clinopyroxene from abyssal peridotites and those from supra-subduction peridotites. REE contents in clinopyroxene are highly sensitive to refertilization processes ([Muntener et al., 2004], [Le Roux et al., 2007] and [Piccardo et al., 2007]). Thus, clinopyroxene can be used as a petrogenetic indicator to characterize the geotectonic setting of ophiolite complexes (Bizimis et al., 2000). In the New Caledonia lherzolites, the clinopyroxene chemistry does not show the LREE inflections observed in the whole rocks (Fig. 8). Niu (2004) made the same observation for abyssal peridotites and proposed two alternative explanations (a) that the ascending melt was too cold to react with the clinopyroxene and instead was trapped as LREE-enriched films along grain boundaries; (b) that only the clinopyroxene rims are affected by melt circulation. Our analyses were made on the cores of the clinopyroxene grains which are unaffected by the refertilization.

The modeling also suggests that the plagioclase lherzolites are more influenced by melt circulation than the spinel lherzolites (~0.1% of melt cf. 0.01%). This is in agreement with previous studies (e.g. [Muntener et al., 2004] and [Piccardo et al., 2007]) that showed that plagioclase lherzolites are hybrid rocks resulting from variable plagioclase addition by percolating melts to pre-existing spinel lherzolites. These conclusions are supported by our spinel compositions (Fig. 7), which are high in Cr compared to the spinel lherzolites. Refertilization has been shown to significantly increase the Cr# in spinel at a given Mg# (Le Roux et al., 2007). Moreover, given that Tartarotti et al. (2002) have demonstrated that high Ti in spinel is related to melt impregnation, the high TiO₂ content also provides evidence of melt circulation.

We therefore propose that the lherzolites of the northern massifs may represent the residue left after the extraction of undepleted MORB melt which was refertilized by the infiltration of a very small amount of LREE-enriched melt ([Navon and Stolper, 1987], [Bodinier et al., 1990], [Takazawa et al., 1992], [Takazawa et al., 2003] and [Li and Lee, 2006]).

4.4.2. U-shaped pattern in harzburgites

The conclusions reached on LREE enrichment of lherzolites can be extended to harzburgites. Indeed, many residues have ratios of light to heavy REE that are too high to be explained in term of residue of equilibrium partial melting ([Prinzhofer and Allegre, 1985] and [Nicolas, 1989]). U-shaped REE patterns are not only observed in the New Caledonia ophiolite, but also in parts of the Othris ophiolite (Barth et al., 2008), the Yarlung Zangbo ophiolite (Dubois-Cote et al., 2005), and the Trinity ophiolite (Gruau et al., 1998). At least three distinct mechanisms have been proposed to account for U-shaped patterns; (i) sequential disequilibrium melting (Prinzhofer and Allegre, 1985), (ii) mantle metasomatism (e.g. Bodinier et al., 1990) and (iii) contamination by crustal sources (e.g. Gruau et al., 1998 and references herein).

Prinzhofer and Allegre (1985) explain the U-shaped pattern on the New Caledonia peridotites by melting that began in the garnet field and finished in the plagioclase field. Although this model is mathematically consistent, it is physically improbable, as partial melting of

peridotites typically never occurs in the plagioclase field (Niu, 2004). Gruau et al. (1998) proposed contamination by crustal materials on the basis of Sr and Nd isotope data. The New Caledonia peridotites are too depleted to measure Sr and Nd isotopic compositions and we cannot use this approach. Nevertheless, a metasomatic event represents a good alternative to explain the LREE enrichment observed in harzburgites and dunites, as fluid migration is very common in subduction zones ([Stolper and Newman, 1994], [Bizimis et al., 2000] and [Dubois-Cote et al., 2005]). It is possible that the fluid was derived in part from continental sediment, in accord with Gruau et al.'s (1998) model.

REE behavior in such environment is difficult to reproduce with a classical batch-melting model, because of the numerous components that could contribute to the REE budget (e.g. fluid from various types of sediment or from fresh or serpentinized basalt and peridotite). In peridotites from both Massif du Sud and Koniambo massif, MREE are 10 times more depleted than HREE in lherzolites. Accounting for such depletion with a simple batch-melting model requires a degree of melting of at least 30%, which is unrealistic in a forearc environment. Furthermore, neither batch melting nor fractional melting can account for U-shaped patterns (Prinzhofer and Allegre, 1985). Such depletion requires at least two stages of partial melting. Bizimis et al. (2000) modeled hydrous melting using a dynamic melting model to account for the REE budget of clinopyroxenes in peridotites from the supra-subduction ophiolitic complex on the Hellenic Peninsula. The model was also used to explain the U-shaped pattern of peridotites from the Vourinos ophiolite and from the Metalleio, Eretria, and eastern Katáchloron sub-massifs (Othris ophiolite) (Barth et al., 2008). Although it reproduces the MREE and HREE contents, the hydrous melting model gives lower LREE contents than observed, which implies that the depleted source and/or hydrous fluids are more enriched in LREE than those used in their model.

From our modeling we conclude that the chemical features of forearc peridotites are best explained with low to medium degrees of hydrous melting of a refertilized source that has previously experienced about 20% of dry melting (Fig. 10C, D). The compositions of peridotites with negative Eu anomalies are reproduced in a model involving the partial melting in the presence of highly LREE enriched fluid following Stolper and Newman (1994). The peridotites with positive Eu anomalies, in contrast, are explained by the infiltration of Eu-enriched hydrous fluid as proposed by Bizimis et al. (2000). The relatively poor fit of the model with the data in Fig. 10C is attributed to a difference in composition between modeled fluid from Bizimis et al. (2000) and the fluid that circulated through the forearc mantle. The real fluid was probably closer in composition to the fluid modeled by Stolper and Newman (1994) (Fig. 10D).

Melts that result from this type of melting display U-shaped REE patterns similar to those of boninites. This observation is consistent with previous studies that demonstrated that boninites are generated by hydrous melting of refractory peridotite (e.g. [Crawford et al., 1981], [Bizimis et al., 2000] and [Arndt, 2003]). A link between boninites and harzburgites in New Caledonia is strongly supported by the study from Marchesi et al. (2009) which shown that ultra-depleted, boninite-type, melts were at the origin of the gabbroic cumulates of the Massif du Sud.

In our model, we conclude that most of New Caledonia ophiolite (e.g. the Massif du Sud and the Koniambo Massif) resulted from a second stage of partial melting of a source that had already experienced MORB depletion. This source is comparable to that of the lherzolites that form the northernmost massifs (Tiebaghi and Poum massifs).

5. Implications of the geochemical model for the geodynamical constraints

Previous studies show that two periods can be distinguished within the tectonic evolution of the Southwest Pacific ([Cluzel et al., 1994], [Cluzel et al., 2001], [Aitchison et al., 1995], [Auzende et al., 1995], [Ali and Aitchison, 2000] and [Auzende et al., 2000]). The period from the Campanian to Paleocene is marked by the opening of marginal basins followed by a convergence during the Eocene. Our results suggest that the mantle section of the New Caledonia ophiolite has recorded two distinct melting stages, i.e., dry melting consistent with an oceanic ridge environment, and hydrous melting is related to a supra-subduction environment. This implies some modifications of the previous model proposed by (Cluzel et al., 2001) and (Whattam et al., 2008). We therefore suggest the following scenario for the evolution of the Norfolk Ridge-Loyalty arc system.

Campanian to Paleocene: The opening of the South Loyalty Basin started at ca. 83 Ma (Fig. 11A), with the production of both the undepleted MORB that dominate the Poya terrane ([Aitchison et al., 1995], [Eissen et al., 1998] and [Cluzel et al., 2001]) and the associated lherzolite residue.

Eocene: The BABB of the Poya Terrane are younger (Mid-Eocene) than most of the undepleted MORB (Campanian to Late Paleocene) and in contrast with the latter, display the isotopic signature of depleted mantle (Cluzel et al., 2001). Nevertheless, both erupted in the same basin (Eissen et al., 1998). Although the occurrence of BABB is considered as a minor feature, the coexistence of BABB and MORB illustrates the heterogeneity of their mantle source, the origin of which remains problematical. Eissen et al. (1994) made similar observations in the North Fiji Basin and postulated interference between an enriched plume-like and a normal shallow source. The slight depletion in Nb–Ta of the back-arc basin tholeiites may result from formation from a mantle source previously affected by supra-subduction processes.

The period of convergence, which started at the Paleocene–Eocene boundary (ca. 55 Ma), is marked by the emplacement of slab melts within the ophiolite (Cluzel et al., 2006) (Fig. 11C). The driving mechanisms responsible for the initiation of the NE-dipping subduction in the South Loyalty Basin remain unclear, because the opening of both Tasman Sea and New Caledonia Basin was completed at this time ([Aitchison et al., 1995] and [Cluzel et al., 2001]). Eissen et al. (1998) proposed that opening of the North Loyalty basin combined with northward motion of the Australian plate generated the regional compression responsible to the inception of the NE-dipping subduction. Crawford et al. (2003), in contrast, proposed that reactivation of a recently extinct spreading ridge accounted for the inception of subduction. Based on this hypothesis, Whattam et al. (2008) suggested that the BABB represent proto-forearc crust that formed after the inception of the NE-dipping subduction at the spreading ridge axis. In fact, there is abundant evidence for the initiation of this subduction at or next the axis of the South Loyalty ridge. The occurrence of both abyssal- and supra-subduction peridotites within the same ophiolite is usually explained by intra-oceanic thrusting and forced subduction at a mid-ocean ridge (e.g. [Insergueix-Filippi et al., 2000], [Barth et al., 2008] and [Dilek et al., 2008]). The coexistence of contemporaneous ridge volcanism and arc-related magmatism in New Caledonia also argue for this hypothesis. Moreover, the position of the Poya terrane as the accretionary prism of the NE-dipping subduction probably results from the difficulty of subducting young and thus hot lithosphere.

It is possible that the refertilization process that affected the lherzolites could have occurred during the conversion of the spreading center to the east-dipping subduction zone (Fig. 11B). Previous studies have shown that refertilized peridotites exhumed in spreading ridges formed during magma-poor periods when liquids stagnate and react with the surrounding mantle (Muntener et al., 2004). Models of subduction inception at spreading centres suggest that MORB magmatic activity does not stop abruptly but progressively decreases (Insergueix-Filippi et al., 2000).

The complete cessation of MORB magmatism is followed by the production of forearc melts (Fig. 11C). Residual high temperatures associated with ridge activity, together with expulsion of hydrous fluid from the slab, lead to the genesis of boninitic melts ([Crawford et al., 1981], [Cameron et al., 1983], [Cameron, 1989], [Insergueix-Filippi et al., 2000], [Arndt, 2003] and [Ishizuka et al., 2006]). Insergueix-Filippi et al. (2000) established that boninitic magmatism starts ca. 3–4 m.y. after the initiation of subduction, and climaxes a few million years later, suggesting that boninites could have erupted in the Paleocene or early Eocene (Fig. 11C). However, boninites can also form during forearc spreading such as that documented in the Hunter Ridge and northern Tonga (Falloon et al., 2008) so that the New Caledonian boninites could potentially have formed at any time between inception of the subduction zone and the obduction of the ophiolite. The small quantity of boninites observed in New Caledonia contrasts with large lava flows expected for this kind of magmatic activity (Arndt, 2003). Likewise, the structural position of the boninites, which are sandwiched between the undepleted MORB and the peridotites, is problematic if we believe that they represent the magmatic crust of the New Caledonia ophiolite. To account for this problem, Crawford et al. (2003) suggested that this crustal section was sliced off as an earlier allochthonous unit that subsequently was over-ridden by the uppermost mantle section (i.e. the ophiolitic nappe). They propose that boninites may have been common throughout the forearc prior to erosion during obduction.

6. Conclusions

Based on our study on four massifs (the Massif du Sud, the Koniambo, the Tiebaghi and the Poum massifs), we infer that the lherzolites from the northern part of the New Caledonia ophiolite may be comparable to abyssal peridotites. These lherzolites likely represent the equilibrium residue of the undepleted MORB terrane formed from Late Cretaceous to Paleocene during the opening of the South Loyalty Basin (Poya terrane). The slowdown of the magmatism activity due to the transition from accretion to convergence in the South Loyalty Basin could be responsible for the refertilization of lherzolites by LREE enriched melts.

The lherzolites underwent a second stage of partial melting during Early Eocene in a forearc environment. This second melting stage is responsible for the genesis of boninitic melts and highly depleted peridotites (i.e. harzburgites) that form the bulk of the ophiolite.

The occurrence of both styles of melting regime — ridge-associated melting and forearc hydrous melting — within the same ophiolite can only be explained by a forced inception of subduction at or near an active spreading center.

Acknowledgements

The analytical work has been supported by the Province Sud de la Nouvelle-Calédonie through funds awarded to Christian Picard during his stay in New Caledonia. We thank Nick

Arndt for its very helpful suggestions and comments on this manuscript. We thank Sarah Bureau and Christèle Poggi for their help during the laboratory and analytical work at the Laboratoire de Géodynamique des Chaînes Alpines, University Joseph Fourier. We thank Francis Coeur for the preparation of rock powders, François Sénebier for mineral separations and Laurence Coogan, Sarah Dare and Andrew Kerr for their very helpful reviews.

References

Ahmed et al., 2005 A.H. Ahmed, S. Arai, Y.M. Abdel-Aziz and A. Rahimi, Spinel composition as a petrogenetic indicator of the mantle section in the Neoproterozoic Bou Azzer ophiolite, Anti-Atlas, Morocco, *Precambrian Research* **138** (3–4) (2005), pp. 225–234.

Aitchison et al., 1995 J. Aitchison, G.L. Clarke, S. Meffre and D. Cluzel, Eocene arc–continent collision in New Caledonia and implications for regional Southwest Pacific tectonic evolution, *Geology* **23** (2) (1995), pp. 161–164.

Ali and Aitchison, 2000 J.R. Ali and J.C. Aitchison, Significance of palaeomagnetic data from the oceanic Poya Terrane, New Caledonia, for SW Pacific tectonic models, *Earth and Planetary Science Letters* **177** (3–4) (2000), pp. 153–161.

Anders and Grevesse, 1989 E. Anders and N. Grevesse, Abundances of the elements: meteoritic and solar, *Geochimica et Cosmochimica Acta* **53** (1) (1989), pp. 197–214.

Arndt, 2003 N. Arndt, Komatiites, kimberlites, and boninites, *Journal of Geophysical Research-Solid Earth* **108** (B6) (2003), pp. 1–11

Audet, 2008 Audet, M.-A., 2008. Caractérisation pétrostructurale et géochimique du massif du Koniambo Nouvelle-Calédonie, PhD., Université du Québec à Montréal, Université de la Nouvelle-Calédonie, Montréal, Nouméa, 281pp.

Auzende et al., 1995 J.-M. Auzende, B. Pelletier and J.-P. Eissen, The North Fiji basin: geology, structure and geodynamic evolution. In: B. Taylor, Editor, *Back-arc basins: Tectonics and Magmatism*, Plenum, NY (1995), pp. 139–175.

Auzende et al., 2000 J.-M. Auzende, S. Van de Beuque, M. Régner, Y. Lafoy and P.A. Symonds, Origin of the New Caledonia ophiolites based on a French–Australian seismic transect, *Marine Geology* **162** (2000), pp. 225–236.

Avias, 1967 J. Avias, Overthrust structure of the main ultrabasic new caledonian massifs, *Tectonophysics* **4** (4-6) (1967), pp. 531–541.

Barrat et al., 1996 J.A. Barrat *et al.*, Determination of rare earth elements in sixteen silicate reference samples by ICP–MS after Tm addition and ion exchange separation, *Geostandards and Geoanalytical Research* **20** (1) (1996), pp. 133–139.

Barth et al., 2008 M.G. Barth, P.R.D. Mason, G.R. Davies and M.R. Drury, The Othris Ophiolite, Greece: a snapshot of subduction initiation at a mid-ocean ridge, *Lithos* **100** (1–4) (2008), pp. 234–254.

Bizimis et al., 2000 M. Bizimis, V.J.M. Salters and E. Bonatti, Trace and REE content of clinopyroxenes from supra-subduction zone peridotites. Implications for melting and enrichment processes in island arcs, *Chemical Geology* **165** (1–2) (2000), pp. 67–85.

Bodinier et al., 1990 J.L. Bodinier, G. Vasseur, J. Vernières, C. Dupuy and J. Fabriès, Mechanisms of mantle metasomatism: geochemical evidence from the Lherz orogenic peridotite, *Journal of Petrology* **31** (3) (1990), pp. 597–628.

Boudier and Nicolas, 1985 F. Boudier and A. Nicolas, Harzburgite and lherzolite subtypes in ophiolitic and oceanic environments, *Earth and Planetary Science Letters* **76** (1–2) (1985), pp. 84–92.

Cameron, 1989 W.E. Cameron, Contrasting tholeiite–boninite associations from New Caledonia. In: A.J. Crawford, Editor, *Boninites*, Uniwin Hyman (1989), pp. 314–338.

Cameron et al., 1983 W.E. Cameron, M.T. McCulloch and D.A. Walker, Boninite petrogenesis: chemical and Nd–Sr isotopic constraints, *Earth and Planetary Science Letters* **65** (1) (1983), pp. 75–89.

Cluzel et al., 1994 D. Cluzel, J. Aitchison, G. Clarke, S. Meffre and C. Picard, Point de vue sur l'évolution tectonique et géodynamique de la Nouvelle–Calédonie, *Comptes Rendus de l'Académie des Sciences* **319** (1994), pp. 683–688.

Cluzel et al., 1997 D. Cluzel, C. Picard, J. Aitchison, C. Laporte, S. Meffre and F. Parat, La nappe de Poya (ex-formation des Basaltes) de Nouvelle–Calédonie (Pacifique Sud-Ouest): un plateau océanique Campanien–Paléocène supérieur obducté à l'Eocène supérieur, *Comptes Rendus de l'Académie des Sciences — Series IIA — Earth and Planetary Science* **324** (6) (1997), pp. 443–451.

Cluzel et al., 2001 D. Cluzel, J.C. Aitchison and C. Picard, Tectonic accretion and underplating of mafic terranes in the Late Eocene intraoceanic forearc of New Caledonia (Southwest Pacific): geodynamic implications, *Tectonophysics* **340** (1–2) (2001), pp. 23–59.

Cluzel et al., 2006 D. Cluzel, S. Meffre, P. Maurizot and A.J. Crawford, Earliest Eocene (53 Ma) convergence in the Southwest Pacific: evidence from pre-obduction dikes in the ophiolite of New Caledonia, *Terra Nova* **18** (6) (2006), pp. 395–402.

Collot et al., 1986 J.-Y. Collot, P. Rigolot and F. Missègue, Geologic structure of the Northern New Caledonia ridge, as inferred from magnetic and gravity anomalies, *Tectonics* **7** (1986), pp. 991–1013.

Collot et al., 1987 J.-Y. Collot, A. Malahoff, J. Recy, G. Latham and F. Missègue, Overthrust emplacement of New Caledonia ophiolite: geophysical evidences, *Tectonics* **6** (1987), pp. 215–232.

Collot and Missègue, 1988 J.-Y. Collot and F. Missègue, Extension de la formation des basaltes de la côte ouest et de la zone d'enracinement des péridotites dans le Grand Lagon Nord de la Nouvelle Calédonie: données géophysiques, *Comptes Rendus de l'Académie des Sciences* **303** (2) (1988), pp. 1437–1442.

Cotten et al., 1995 J. Cotten, A. Le Dez, M. Bau, M. Caroff, R. Maury, P. Dulski, S. Fourcade, M. Bohn and R. Brousse, Origin of anomalous rare-earth element and yttrium enrichments in subaerially exposed basalts: evidence from French Polynesia, *Chemical Geology* **119** (1–4) (1995), pp. 115–138.

Crawford et al., 1981 A.J. Crawford, L. Beccaluva and G. Serri, Tectono-magmatic evolution of the West Philippine–Mariana region and the origin of boninites, *Earth and Planetary Science Letters* **54** (2) (1981), pp. 346–356.

Crawford et al., 2003 A.J. Crawford, S. Meffre and P.A. Symonds, 120 to 0 Ma tectonic evolution of the southwest Pacific and analogous geological evolution of the 600 to 220 Ma Tasman Fold Belt System, *Geological Society of Australia, Special Publication* **22** (2003), pp. 377–397.

Deschamps et al., 2010 F. Deschamps, S. Guillot, M. Godard, C. Chauvel, M. Andreani and K. Hattori, In situ characterization of serpentinites from forearc mantle wedges: Timing of serpentinization and behavior of fluid-mobile elements in subduction zones, *Chemical Geology* **269** (2010), pp. 262–277.

Dick and Bullen, 1984 H. Dick and T. Bullen, Chromian spinel as a petrogenetic indicator in abyssal and alpine-type peridotites and spatially associated lavas, *Contributions to Mineralogy and Petrology* **86** (1984), pp. 54–76.

Dilek et al., 2008 Y. Dilek, H. Furnes and M. Shallo, Geochemistry of the Jurassic Mirdita Ophiolite (Albania) and the MORB to SSZ evolution of a marginal basin oceanic crust, *Lithos* **100** (1–4) (2008), pp. 174–209.

Dubois-Cote et al., 2005 V. Dubois-Cote, R. Hebert, C. Dupuis, C. Wang, Y. Li and J. Dostal, Petrological and geochemical evidence for the origin of the Yarlung Zangbo ophiolites, southern Tibet, *Chemical Geology* **214** (3–4) (2005), pp. 265–286.

Eissen et al., 1998 J.-P. Eissen *et al.*, Geochemistry and tectonic significance of basalts in the Poya Terrane, New Caledonia, *Tectonophysics* **284** (3–4) (1998), pp. 203–219.

Eissen et al., 1994 J.-P. Eissen, M. Nohara, J. Cotten and K. Hirose, North Fiji Basin basalts and their magma sources. Incompatible element constraints, *Marine Geology* **116** (1–2) (1994), pp. 153–178.

Falloon et al., 2008 T.J. Falloon, L.V. Danyushevsky, A.J. Crawford, S. Meffre, J.D. Woodhead and S.H. Bloomer, Boninites and adakites from the northern termination of the Tonga Trench: implications for adakite petrogenesis, *Journal of Petrology* **49** (4) (2008), pp. 697–715.

Fitzherbert et al., 2004 J.A. Fitzherbert, G.L. Clarke, B. Marmo and R. Powell, The origin and P–T evolution of peridotites and serpentinites of NE New Caledonia: prograde interaction between continental margin and the mantle wedge, *Journal of Metamorphic Geology* **22** (4) (2004), pp. 327–344.

- Fitzherbert et al., 2005 J.A. Fitzherbert, G.L. Clarke and R. Powell, Preferential retrogression of high-P metasediments and the preservation of blueschist to eclogite facies metabasite during exhumation, Diahot terrane, NE New Caledonia, *Lithos* **83** (1–2) (2005), pp. 67–96.
- Garbe-Schonberg, 1993 C. Garbe-Schonberg, Simultaneous determination of thirty-seven trace elements in twenty-eight international rock standards by ICP-MS, *Geostandards and Geoanalytical Research* **17** (1) (1993), pp. 81–97.
- Govindaraju, 1995 K. Govindaraju, 1995 working values with confidence limits for twenty-six CRPG, ANRT and IWG-GIT geostandards, *Geostandards Newsletter* **19** (1995), pp. 1–32.
- Gruau et al., 1998 G. Gruau, J. Bernard-Griffiths and C. Lécuyer, The origin of U-shaped rare earth patterns in ophiolite peridotites: assessing the role of secondary alteration and melt/rock reaction, *Geochimica et Cosmochimica Acta* **62** (21–22) (1998), pp. 3545–3560.
- Hattori and Guillot, 2007 K.H. Hattori and S. Guillot, Geochemical character of serpentinites associated with high- to ultrahigh-pressure metamorphic rocks in the Alps, Cuba, and the Himalayas: recycling of elements in subduction zones, *Geochemistry Geophysics Geosystems* **8** (9) (2007).
- Insergueix-Filippi et al., 2000 D. Insergueix-Filippi, L. Dupeyrat, A. Dimo-Lahitte, P. Vergly and J. Bébien, Albanian ophiolites II — model of subduction infancy at a mid-ocean ridge, *Ophioliti* **25** (1) (2000), pp. 47–53.
- Ishii et al., 1992 T. Ishii, P.T. Robinson, H. Mackawa and R. Fiske, Petrological studies of peridotites from diapiric serpentinite seamounts in the Izu-Ogazawara-Mariana forearc, LEG 125, *Proceedings of Ocean Drilling Program, Scientific Results* **125** (1992), pp. 445–485.
- Ishizuka et al., 2006 O. Ishizuka *et al.*, Early stages in the evolution of Izu–Bonin arc volcanism: new age, chemical, and isotopic constraints, *Earth and Planetary Science Letters* **250** (1–2) (2006), pp. 385–401.
- Iyer et al., 2008 K. Iyer, H. Austrheim, T. John and B. Jamtveit, Serpentinization of the oceanic lithosphere and some geochemical consequences: constraints from the Leka Ophiolite Complex, Norway, *Chemical Geology* **249** (1–2) (2008), pp. 66–90.
- Jochum and Nohl, 2008 K.P. Jochum and U. Nohl, Reference materials in geochemistry and environmental research and the GeoReM database, *Chemical Geology* **253** (1–2) (2008), pp. 50–53.
- Johnson and Dick, 1992 K.T.M. Johnson and H.J.B. Dick, Open system melting and temporal and spatial variation of peridotite and basalt at the Atlantis II fracture zone, *Journal of Geophysical Research* **97** (B6) (1992), pp. 9219–9241.
- Johnson et al., 1990 K.T.M. Johnson, H.J.B. Dick and N. Shimizu, Melting in the oceanic upper mantle: an ion microprobe study of diopsides in abyssal peridotites, *Journal of Geophysical Research* **95** (1990), pp. 2661–2678.

Kelemen et al., 1990 P.B. Kelemen, K.T.M. Johnson, R.J. Kinzler and A.J. Irving, High-field-strength element depletions in arc basalts due to mantle–magma interaction, *Nature* **345** (6275) (1990), pp. 521–524.

Langmuir et al., 1977 C. Langmuir, A.F. Bender, A.E. Bence, G.N. Hanson and S. Taylor, Petrogenesis of basalts from the FAMOUS area: Mid-Atlantic Ridge, *Earth and Planetary Science Letters* **36** (1977), pp. 133–156.

Le Roux et al., 2007 V. Le Roux, J. Bodinier, A. Tommasi, O. Alard, J. Dautria, A. Vauchez and A. Riches, The Lherz spinel lherzolite: refertilized rather than pristine mantle, *Earth and Planetary Science Letters* **259** (3–4) (2007), pp. 599–612.

Li and Lee, 2006 Z.-X.A. Li and C.-T.A. Lee, Geochemical investigation of serpentinized oceanic lithospheric mantle in the Feather River ophiolite, California: implications for the recycling rate of water by subduction, *Chemical Geology* **235** (1–2) (2006), pp. 161–185.

Marchesi et al., 2009 C. Marchesi, C. Garrido, M. Godard and F. Belley, Migration and accumulation of ultra-depleted subduction-related melts in the Massif du Sud ophiolite (New Caledonia), *Chemical Geology* **266** (3–4) (2009), pp. 180–195.

McDonough and Sun, 1995 W.F. McDonough and S.S. Sun, The composition of the Earth, *Chemical Geology* **120** (3–4) (1995), pp. 223–253.

Moutte, 1979 J. Moutte, Le massif de Tiébaghi, Nouvelle Calédonie, et ses gîtes de chromite, L'Ecole Nationale des Mines, Paris (1979) 172pp..

Muntener et al., 2004 O. Muntener, T. Pettke, L. Desmurs, M. Meier and U. Schaltegger, Refertilization of mantle peridotite in embryonic ocean basins: trace element and Nd isotopic evidence and implications for crust–mantle relationships, *Earth and Planetary Science Letters* **221** (1–4) (2004), pp. 293–308.

Navon and Stolper, 1987 O. Navon and E. Stolper, Geochemical consequences of melt percolation: the upper mantle as chromatographic column, *Journal of Geology* **95** (1987), pp. 285–308.

Nicolas, 1989 A. Nicolas, Structures of ophiolites and dynamics of oceanic lithosphere, Kluwer, Dordrecht (1989) 368pp..

Nicolas and Boudier, 2003 A. Nicolas and F. Boudier, Where ophiolites come from and what they tell us, *Ophiolite concept and the evolution of geological thought*, *Geological Society of America Special Paper* **373** (2003), pp. 137–152.

Nicolas and Dupuy, 1984 A. Nicolas and C. Dupuy, Origin of ophiolitic and oceanic lherzolites, *Tectonophysics* **110** (3–4) (1984), pp. 177–187.

Niu, 1997 Y. Niu, Mantle melting and melt extraction processes beneath ocean ridges: evidence from abyssal peridotites, *Journal of Petrology* **38** (8) (1997), pp. 1047–1074.

Niu, 2004 Y. Niu, Bulk-rock Major and trace element compositions of abyssal peridotites: implications for mantle melting, melt extraction and post-melting processes beneath mid-ocean ridges, *Journal of Petrology* **45** (12) (2004), pp. 2423–2458.

Niu and Hékinian, 1997 Y. Niu and R. Hékinian, Basaltic liquids and harzburgitic residues in the Garrett Transform: a case study at fast-spreading ridges, *Earth and Planetary Science Letters* **146** (1–2) (1997), pp. 243–258.

Niu et al., 1997 Y. Niu, C.H. Langmuir and R.J. Kinzler, The origin of abyssal peridotites: a new perspective, *Earth and Planetary Science Letters* **152** (1–4) (1997), pp. 251–265.

Paris, 1981 J.P. Paris, Géologie de la Nouvelle-Calédonie : Un essai de synthèse, Bureau de Recherches Géologiques et Minières, Orléans (1981) 267pp.

Parkinson et al., 1992 I.J. Parkinson, J.A. Pearce, M.F. Thirlwall, K.T.M. Johnson and G. Ingram, Trace element geochemistry of peridotites from the Izu–Bonin–Mariana forearc, LEG 125, *Proceedings of Ocean Drilling Program, Scientific Results* **125** (1992), pp. 487–506.

Piccardo et al., 2007 G.B. Piccardo, A. Zanetti and O. Muntener, Melt/peridotite interaction in the Southern Lanzo peridotite: field, textural and geochemical evidence, *Lithos* **94** (1–4) (2007), pp. 181–209.

Prinzhofer, 1981 Prinzhofer, A., 1981. Structure et pétrologie d'un cortège ophiolitique : Le Massif du Sud (Nouvelle–Calédonie). La transition manteau-croûte en milieu océanique, Ecole Normale Supérieure des Mines, Paris, 185pp.

Prinzhofer and Allegre, 1985 A. Prinzhofer and C.J. Allegre, Residual peridotites and the mechanisms of partial melting, *Earth and Planetary Science Letters* **74** (2–3) (1985), pp. 251–265.

Rawling and Lister, 2002 T.J. Rawling and G.S. Lister, Large-scale structure of the eclogite-blueschist belt of New Caledonia, *Journal of Structural Geology* **24** (8) (2002), pp. 1239–1258.

Sameshima et al., 1983 T. Sameshima, J.P. Paris, P.M. Black and R.F. Heming, Clinoenstatite-bearing lava from Nepoui, New Caledonia, *American Mineralogist* **68** (11–12) (1983), pp. 1076–1082.

Sécher, 1981 D. Sécher, Les lherzolites ophiolitiques de la Nouvelle–Calédonie et leurs gisements de chromites, Université de Nantes, Nantes (1981) 300pp..

Shaw, 1970 D.M. Shaw, Trace element fractionation during anatexis, *Geochimica et Cosmochimica Acta* **34** (1970), pp. 237–243.

Shaw, 2000 D.M. Shaw, Continuous (dynamic) melting theory revisited, *Can. Mineral* **38** (5) (1970), p. 1041.

Spandler et al., 2004 C. Spandler, J. Hermann, R. Arculus and J. Mavrogenes, Geochemical heterogeneity and element mobility in deeply subducted oceanic crust; insights from high-pressure mafic rocks from New Caledonia, *Chemical Geology* **206** (1–2) (2004), pp. 21–42.

Spandler et al., 2005 C. Spandler, D. Rubatto and R. Hermann, Late Cretaceous–Tertiary tectonics of the southwest Pacific: insights from U–Pb sensitive, high-resolution ion microprobe (SHRIMP) dating of eclogite facies rocks from New Caledonia, *Tectonics* **24** (3) (2005), p. 16.

Stolper and Newman, 1994 E. Stolper and S. Newman, The role of water in the petrogenesis of Mariana trough magmas, *Earth and Planetary Science Letters* **121** (3–4) (1994), pp. 293–325.

Takazawa et al., 1992 E. Takazawa, F.A. Frey, N. Shimizu, M. Obata and J.L. Bodinier, Geochemical evidence for melt migration and reaction in the upper mantle, *Nature* **359** (1992), pp. 55–58.

Takazawa et al., 2000 E. Takazawa, F.A. Frey, N. Shimizu and M. Obata, Whole rock compositional variations in an upper mantle peridotite (Horoman, Hokkaido, Japan): are they consistent with a partial melting process?, *Geochimica et Cosmochimica Acta* **64** (4) (2000), pp. 695–716.

Takazawa et al., 2003 E. Takazawa, T. Okayasu and K. Satoh, Geochemistry and origin of the basal lherzolites from the northern Oman ophiolite (northern Fizeh block), *Geochemistry Geophysics Geosystems* **4** (2) (2003).

Tartarotti et al., 2002 P. Tartarotti, S. Susini, P. Nimis and L. Ottolini, Melt migration in the upper mantle along the Romanche Fracture Zone (Equatorial Atlantic), *Lithos* **63** (3–4) (2002), pp. 125–149.

Whattam, 2008 S.A. Whattam, Arc–continent collisional orogenesis in the SW Pacific and the nature, source and correlation of emplaced ophiolitic nappe components, *Lithos* **113** (2008), pp. 88–114.

Whattam et al., 2008 S.A. Whattam, J. Malpas, J.R. Ali and I.E.M. Smith, New SW Pacific tectonic model: cyclical intraoceanic magmatic arc construction and near-coeval emplacement along the Australia–Pacific margin in the Cenozoic, *Geochemistry Geophysics Geosystems* **9** (3) (2008).

You et al., 1996 C.F. You, P.R. Castillo, J.M. Gieskes, L.H. Chan and A.J. Spivack, Trace element behavior in hydrothermal experiments: Implications for fluid processes at shallow depths in subduction zones, *Earth and Planetary Science Letters* **140** (1–4) (1996), pp. 41–52.

Figures

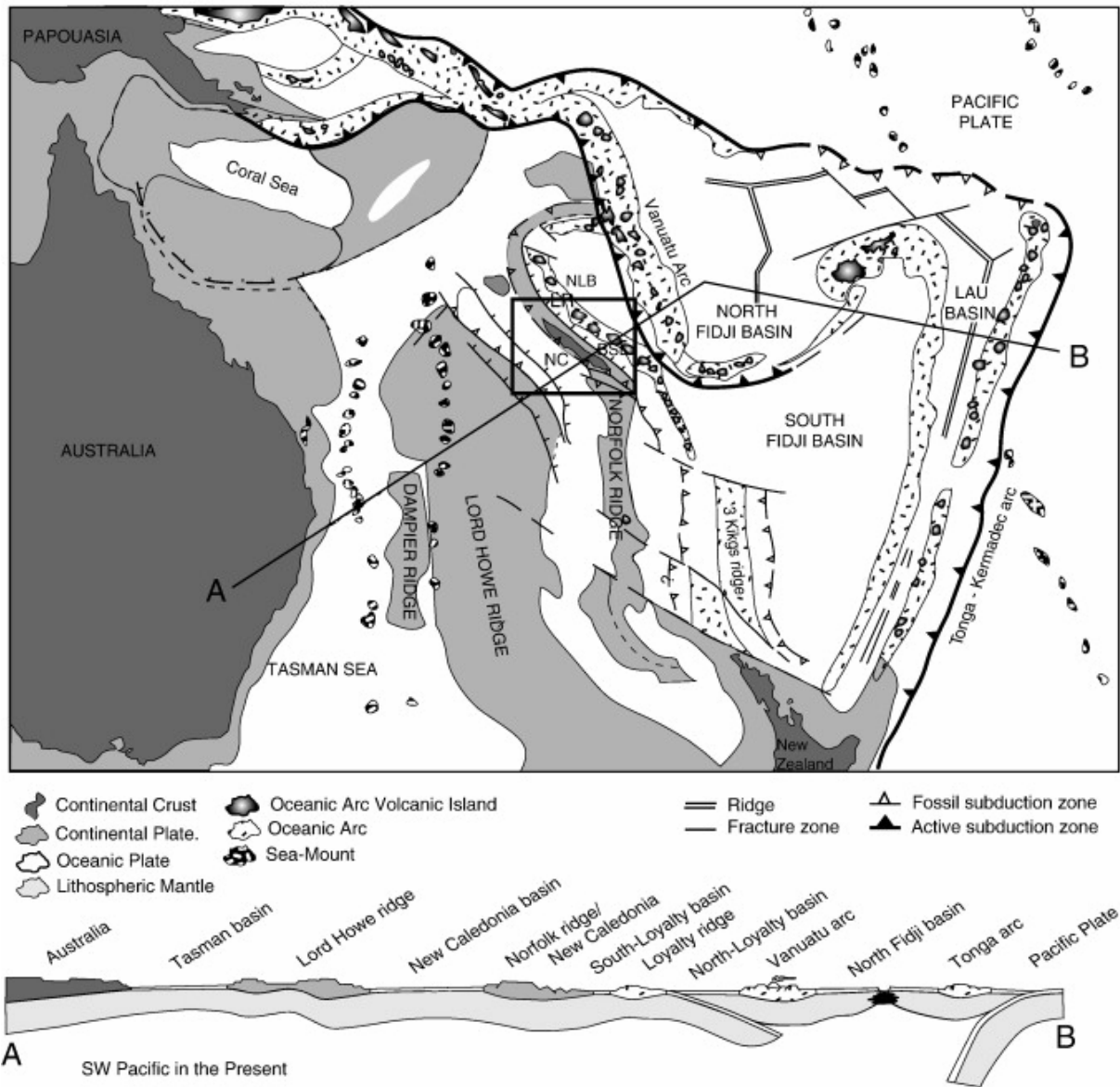


Fig. 1. Structural map of Southwest Pacific (modified from Cluzel et al., 2001). NC: New Caledonia ; SLB : South Loyalty Basin ; NLB : North Loyalty Basin.

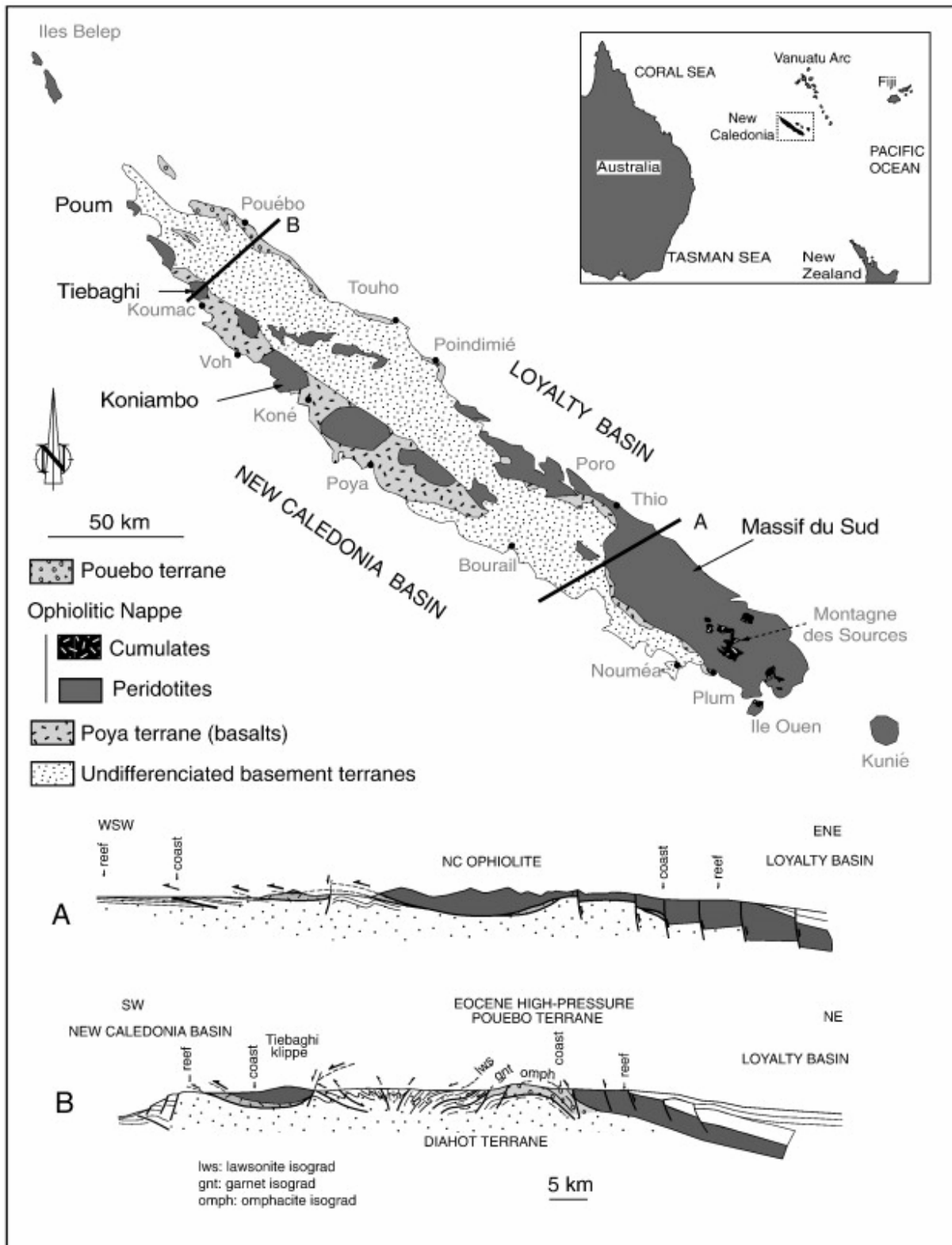


Fig. 2. Simplified geological map of the New Caledonia, showing the localization of the ophiolitic massifs presented in this study. The Pouébo terrane (not developed in this paper) consists of a melange of eclogite-facies magmatic rocks genetically related to the Poya terrane which were metamorphosed in the northeast dipping subduction ([Cluzel et al., 1994], [Cluzel et al., 2001], [Rawling and Lister, 2002], [Fitzherbert et al., 2004], [Spandler et al., 2004], [Spandler et al., 2005] and [Fitzherbert et al., 2005]).

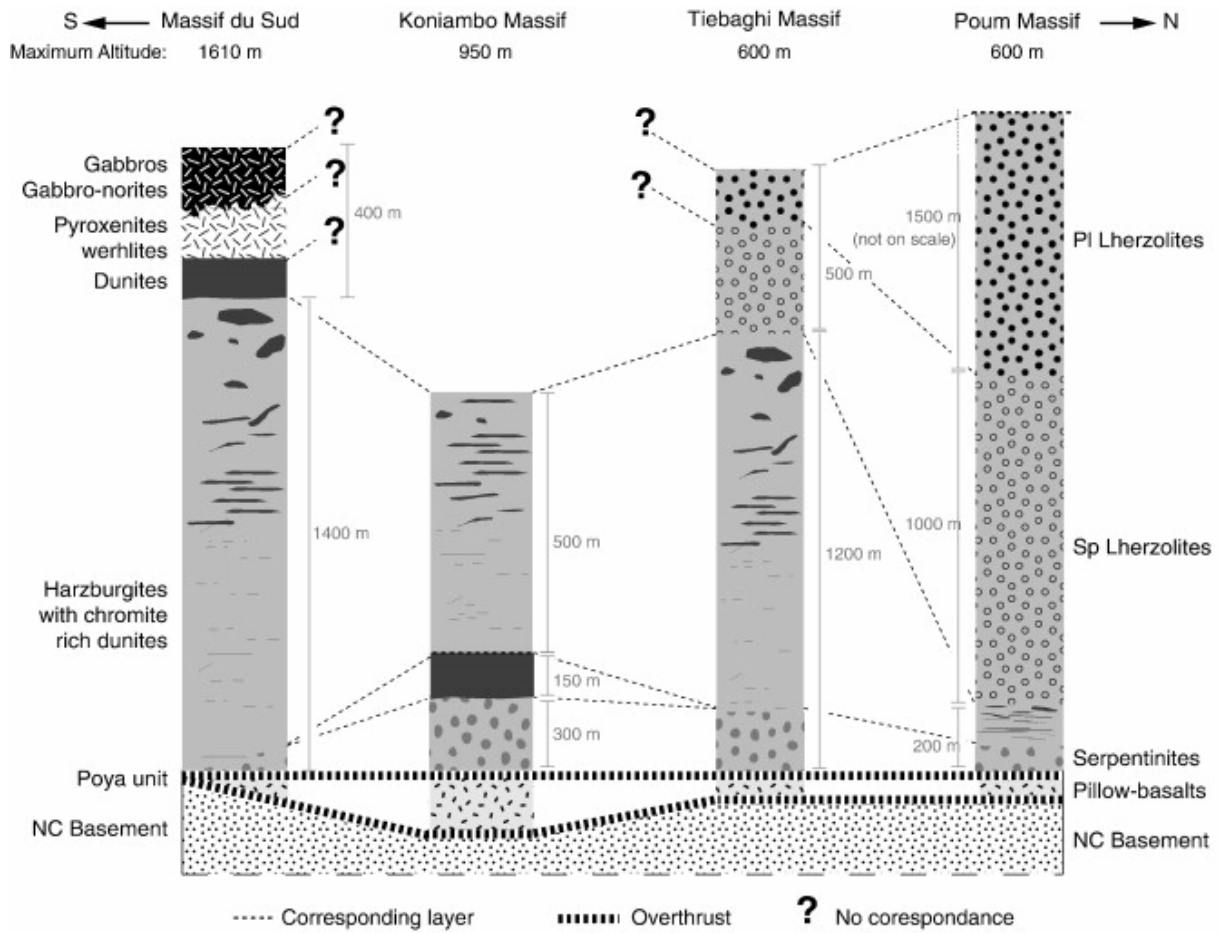


Fig. 3. Comparative and schematic stratigraphy column of the four studied massifs : the Massif du Sud, the Koniambo massif, the Tiebaghi massif and the Poum massif. Approximative thicknesses and maximum altitude are from (Prinzhofer, 1981), (Audet, 2008), (Moutte, 1979) and (Sécher, 1981).

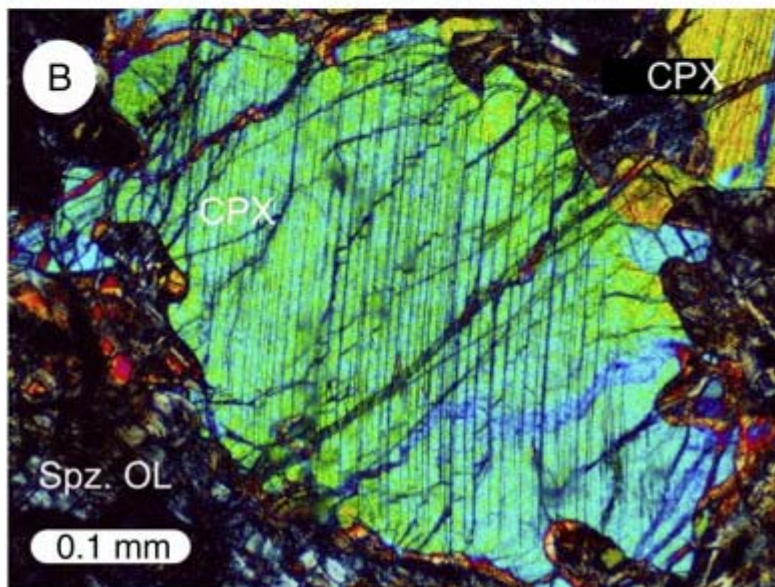
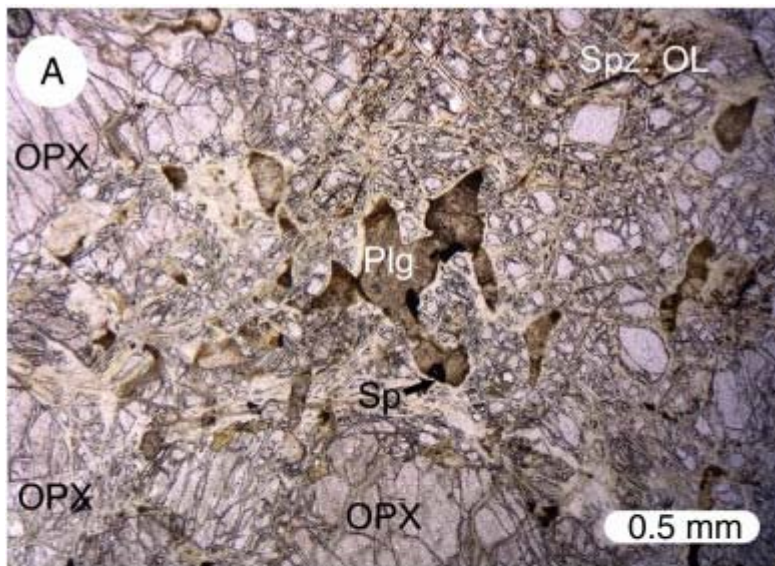


Fig. 4. Microtextures of plagioclase ilherzolite from the Poum massif and spinel ilherzolite from the Tiebaghi massif. A: Interstitial plagioclase between serpentinized olivine. B: Clinopyroxene with lobate rims in spinel ilherzolite (Spz Ol: Serpentinized olivine; OPX: Orthopyroxene; CPX: Clinopyroxene; Sp: Spinel; Plg: Plagioclase).

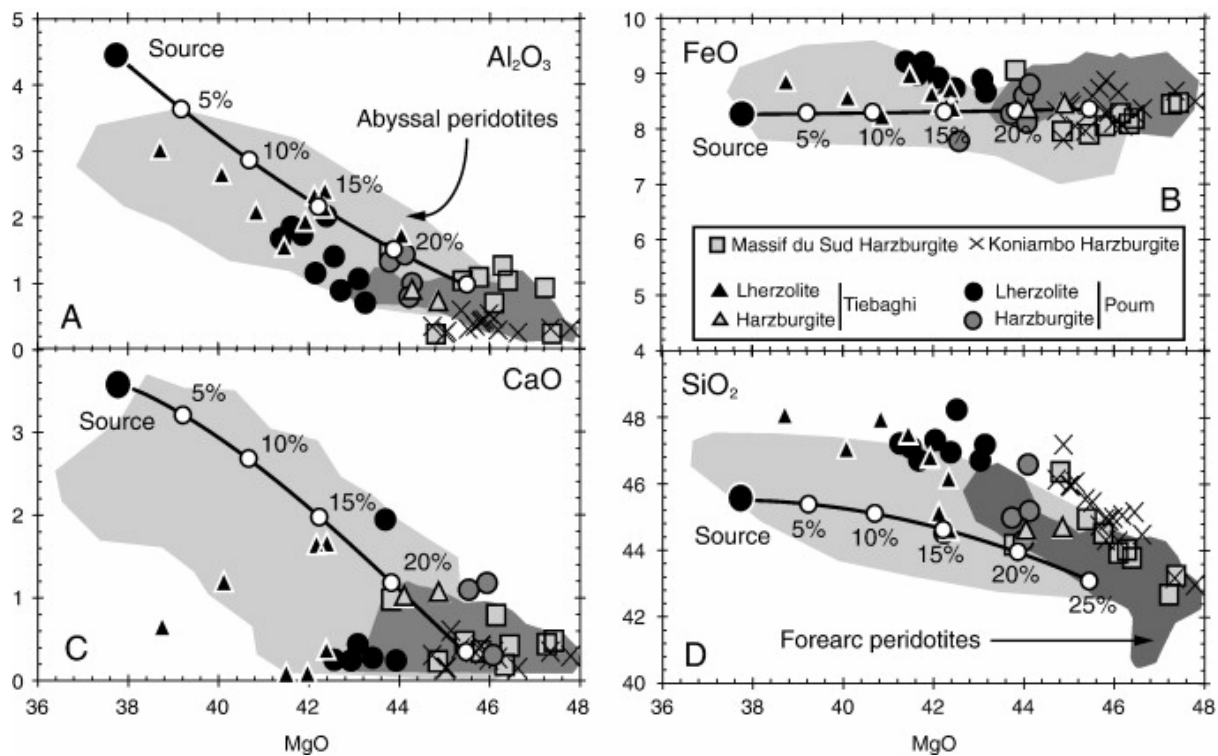


Fig. 5. Major oxides vs. MgO diagrams for whole rocks of New Caledonia peridotites compared with calculated trends for residual peridotites using the model of Niu (1997). Element concentrations are recalculated to 100% on LOI-free basis. Data sources for abyssal peridotites and supra-subduction peridotites are from Niu (2004) and from Ishii et al. (1992) respectively. Source end-member is from McDonough and Sun (1995). The melting calculation assumed polybaric near-fractional melting of a spinel peridotite from 2.5 GPa to 0.4 GPa. Numbers along the trends correspond to percent melting.

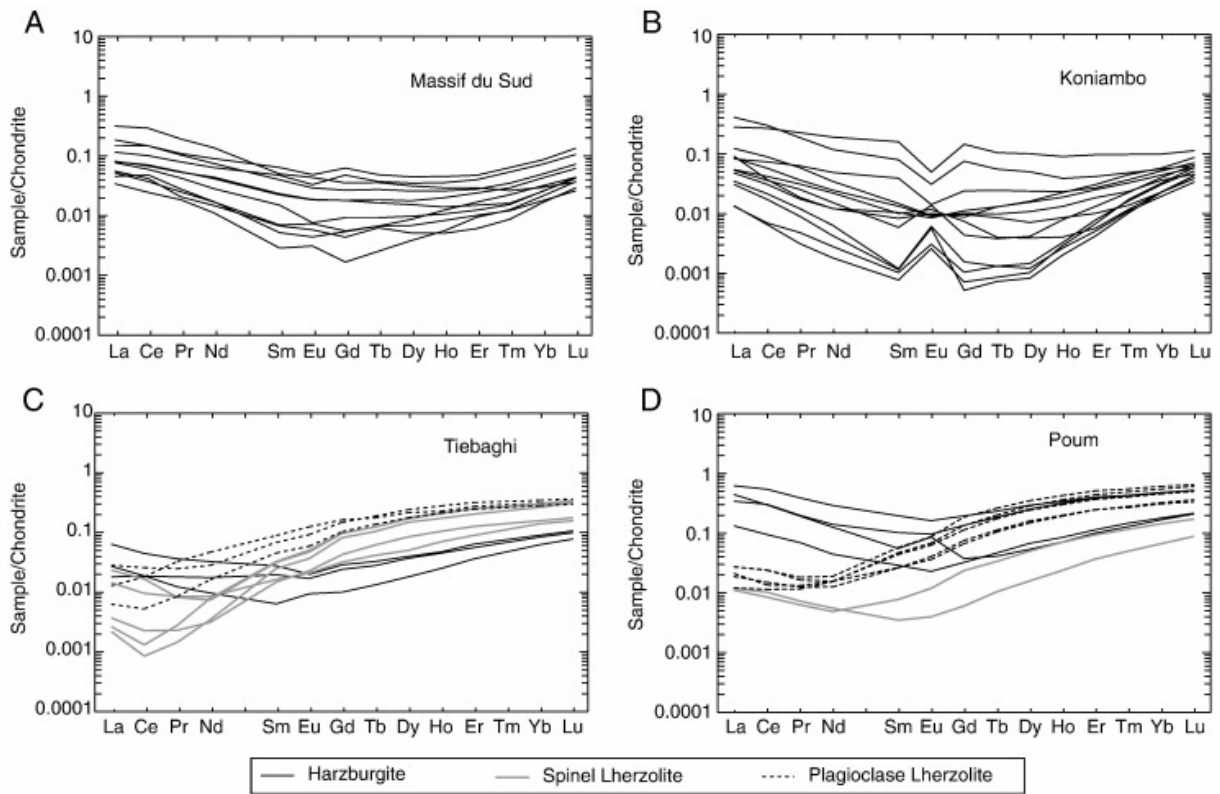


Fig. 6. Chondrite C1-normalized REE diagram for whole rock compositions of New Caledonia peridotites. (A) peridotites from the Massif du sud, (B) peridotites from the Koniambo massif, (C) Peridotites from the Tiebaghi massif, and (D) peridotites from the Poum massif. Chondritic values are from Anders and Grevesse (1989).

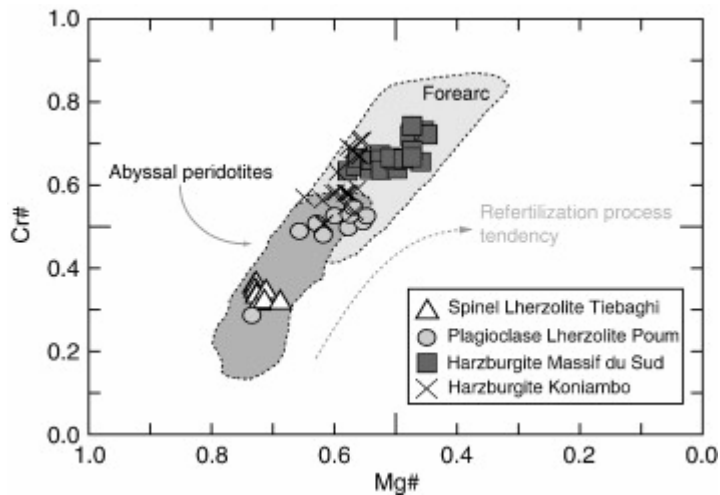


Fig. 7. Cr# vs. Mg# from chromian spinels. Cr# and Mg# correspond respectively to $\text{Cr}/(\text{Cr} + \text{Al})$ and $\text{Mg}/(\text{Mg} + \text{Fe}^{2+})$. Forearc peridotites are from Ishii et al. (1992) and abyssal peridotites are from Dick and Bullen (1984). Grey arrow indicates expected behavior of spinels from refertilized rocks (Le Roux et al., 2007).

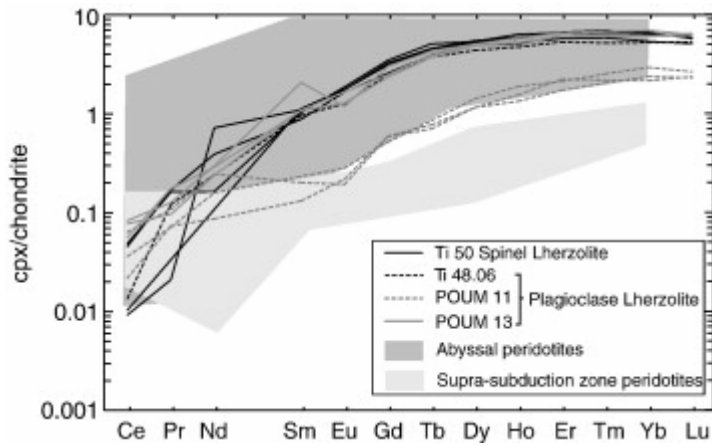


Fig. 8. Chondrite C1-normalized REE patterns for the clinopyroxene from the northern massifs of New Caledonia. Clinopyroxene fields are from (Johnson et al., 1990) and (Johnson and Dick, 1992) for abyssal peridotites, and from Parkinson et al. (1992) for supra-subduction peridotites. Normalized as in Fig. 6.

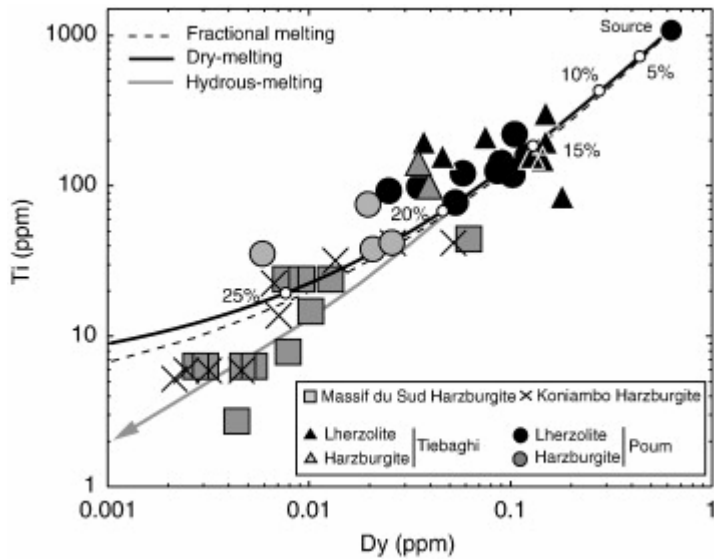


Fig. 9. Ti vs. Dy concentrations (in ppm). Dry melting trend shows residual compositions during dry melting (incremental non-modal batch melting at 0.1% increments) of a MORB source (from McDonough and Sun, 1995). Fractional melting model from Shaw (1970) is shown for comparison. Hydrous melting trend shows residual peridotite composition during hydrous melting using the model of Bizimis et al. (2000). The source is a residue of 18% dry melting of the MORB source. Numbers along the line indicate percent melting.

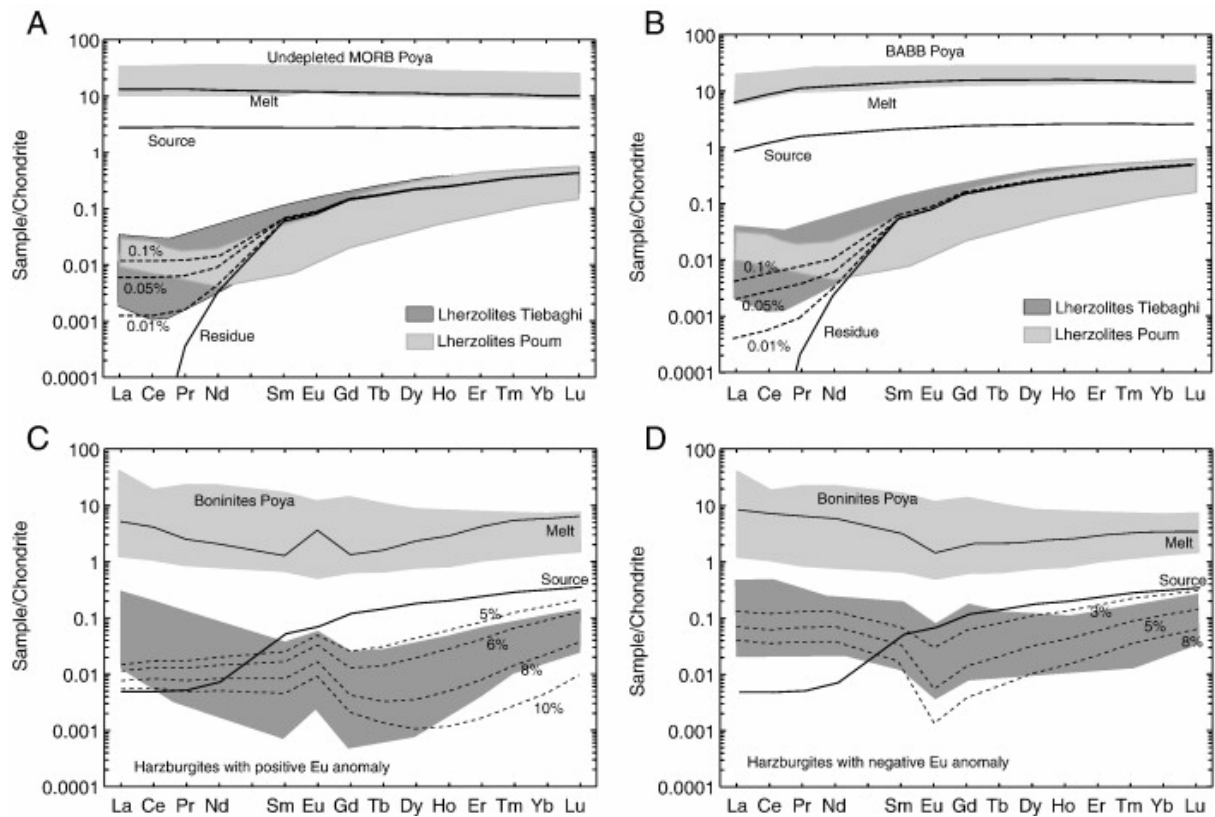


Fig. 10. Results of chondrite C1-normalized REE modeling using dry melting followed by melt–rock interaction (a, b) and hydrous melting (c, d). All parameters used in these models are in Table 4. A: melt extracted from an enriched mantle source reacts with a residue of 18% melting. Ascending liquids from the deeper and more fertile part of the mantle react with a depleted peridotite in shallower parts of the mantle. The enriched mantle source corresponds to the pyrolite calculated by McDonough and Sun (1995). The undepleted MORB Poya field is from Cluzel et al. (2001). Percents indicate melt proportions used to refertilize the residue. B: Dry melting as in A, using a depleted mantle source. Depleted mantle source is from Niu and Hékinian (1997), and BABB Poya field is from Cluzel et al. (2001). C: Hydrous melting of a MORB depleted source that has experienced LREE enriched melt circulation (melt/peridotite ratio of 0.05%, first melting stage is estimated to 18%). Dashed lines show hydrous melting using the maximum concentrations in the fluid component calculated by Bizimis et al. (2000). Calculated melt is obtained with 5% of partial melting. New Caledonia boninite field is from (Cameron, 1989) and (Audet, 2008). Numbers along the line indicate percent melting of the second partial melting stage. D: Hydrous melting as C, using calculated hydrous fluid from Stolper and Newman (1994). Normalized as in Fig. 6.

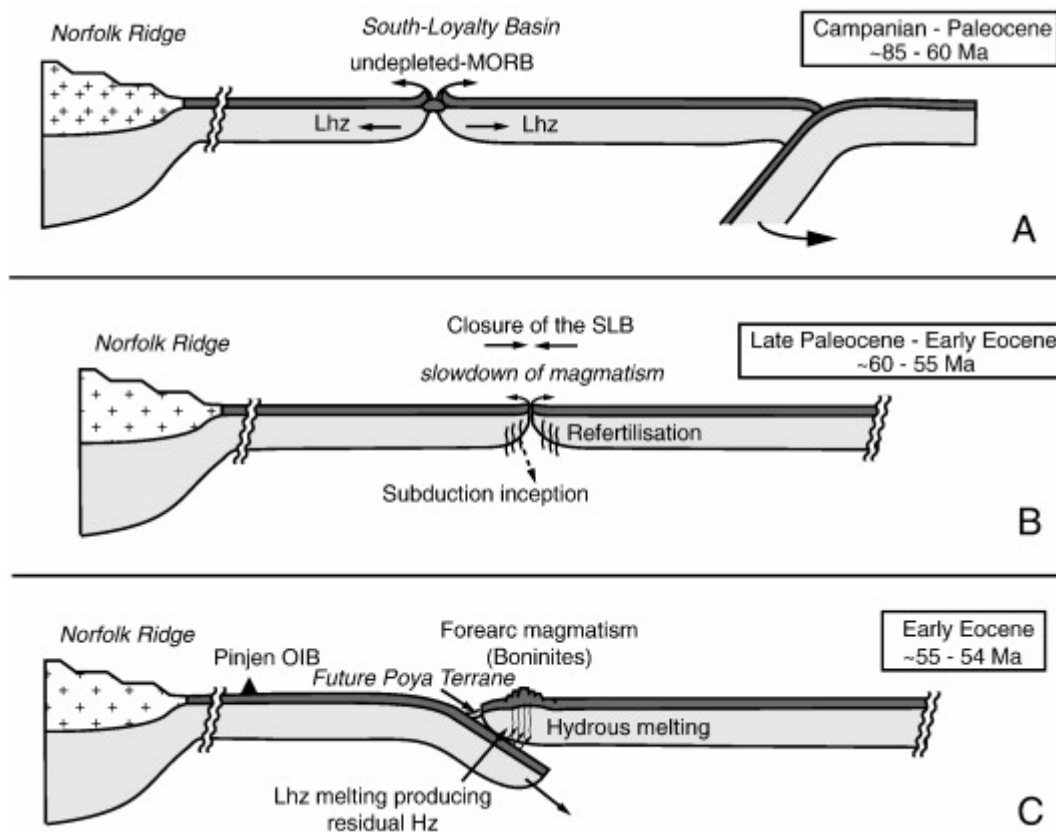


Fig. 11. Profile sketch of the Campanian (A) to Mid-Eocene (C) evolution of the South Loyalty Basin (see text for more details). A: Campanian to Paleocene. Opening of the South Loyalty Basin, with the formation of undepleted MORB with equilibrium residue (lhz: lherzolite), associated with the slab withdrawal east to the Gondwana margin. B: Late Paleocene to Early Eocene. The closure of the South Loyalty Basin leads to the refertilization process affecting the depleted lherzolites. The NE-dipping subduction starts at (or near) the spreading ridge center. C: Early Eocene to Mid-Eocene. The ~ 55 age corresponds to the inception of the subduction, with associated forearc magmatism. The dehydration of the slab is responsible for the second stage of partial melting of the forearc peridotites (residual harzburgites, i.e. the future New Caledonia ophiolite), probably forming boninitic melts. The future Poya terrane corresponds to the accretionary prism linked to the NE-dipping subduction.

Table 1. Whole rock major and rare earth elements of the New Caledonia peridotites (< D.L.: Lower than the detection limit). REF.: References, corresponding to [Govindaraju \(1995\)](#) for major element concentrations and to [Garbe-Schonberg \(1993\)](#) for REE concentration (RSD: Relative Standard Deviation). Complete data are available online as a supplementary table.

Sample	xx3127	xx3131	Yaté 1	POR 6	POR 11	Ti 2	Ti 48-06	Ti 50	Pou m 2	Pou m 3
Location	Koniambo	Koniambo	Massif du Sud	Massif du Sud	Massif du Sud	Tiébaghi	Tiébaghi	Tiébaghi	Pou m	Pou m
Nature	Hz	Hz	Hz	Hz	Hz	Lhz	Lhz	Lhz	Lhz	Lhz
SiO ₂ (wt.%)	40.18	40.81	39.78	43.99	44.85	40.51	40.61	40.80	39.72	39.26
TiO ₂	0.002	0.003	0.001	0.001	0.004	0.030	0.013	0.014	0.020	0.010
Al ₂ O ₃	0.25	0.54	1.14	1.04	1.03	1.51	1.52	1.64	1.62	1.08
FeOT	7.37	7.13	7.32	8.23	7.89	8.36	7.67	7.68	7.76	7.77
MnO	0.11	0.10	0.10	0.12	0.12	0.12	0.11	0.11	0.11	0.11
MgO	39.38	40.63	41.96	46.77	45.45	38.70	38.09	38.55	37.52	38.86
CaO	0.14	0.36	0.14	0.40	0.44	1.67	1.48	1.53	1.85	1.17
Na ₂ O	< D.L.	<D.L.	0.01	<D.L.	<D.L.	0.01	<D.L.	<D.L.	0.02	<D.L.
K ₂ O	<D.L.	<D.L.	0.01	<D.L.	<D.L.	0.01	<D.L.	<D.L.	<D.L.	<D.L.
P ₂ O ₅	<D.L.	<D.L.	0.00	0.06	0.13	<D.L.	<D.L.	<D.L.	0.13	<D.L.
LOI	10.80	9.78	8.67	0.19	0.13	9.01	9.60	9.15	11.33	11.34
SUM	98.23	99.33	99.15	100.79	100.04	99.93	99.08	99.47	99.93	99.61
La (ppm)	0.0112	0.0174	0.0175	0.0185	0.0418	0.0080	0.0014	0.0145	0.0067	0.0066
Ce	0.0139	0.0404	0.0350	0.0398	0.0864	0.0290	0.0014	0.0268	0.0150	0.0152
Pr	0.0013	0.0052	0.0038	0.0047	0.0092	0.0080	0.0004	0.0020	0.0017	0.0016

Sample	xx3127	xx3131	Yaté 1	POR 6	POR 11	Ti 2	Ti 48-06	Ti 50	Pou m 2	Pou m 3
Location	Koniambo	Koniambo	Massif du Sud	Massif du Sud	Massif du Sud	Tiébaghi	Tiébaghi	Tiébaghi	Pou m	Pou m
Nature	Hz	Hz	Hz	Hz	Hz	Lhz	Lhz	Lhz	Lhz	Lhz
Nd	0.0055	0.0200	0.0124	0.0193	0.0327	0.0560	0.0042	0.0089	0.0089	0.0074
Sm	0.0021	0.0052	0.0021	0.0033	0.0057	0.0345	0.0097	0.0123	0.0088	0.0041
Eu	0.0009	0.0007	0.0004	0.0010	0.0016	0.0183	0.0054	0.0070	0.0050	0.0021
Gd	0.0032	0.0043	0.0018	0.0034	0.0051	0.0847	0.0425	0.0503	0.0378	0.0136
Tb	0.0007	0.0008	0.0003	0.0006	0.0010	0.0166	0.0098	0.0117	0.0096	0.0039
Dy	0.0056	0.0052	0.0023	0.0036	0.0061	0.1380	0.0954	0.1130	0.0877	0.0373
Ho	0.0015	0.0011	0.0006	0.0007	0.0014	0.0323	0.0245	0.0301	0.0236	0.0107
Er	0.0056	0.0039	0.0019	0.0023	0.0043	0.1140	0.0850	0.1050	0.0834	0.0402
Tm	0.0010	0.0008	0.0004	0.0004	0.0008	0.0184	0.0147	0.0175	0.0139	0.0071
Yb	0.0086	0.0075	0.0040	0.0039	0.0077	0.1310	0.1110	0.1270	0.0999	0.0531
Lu	0.0017	0.0016	0.0010	0.0010	0.0017	0.0208	0.0201	0.0219	0.0163	0.0091

Table 2. Spinel major element analyses of NC peridotites (Hz: harzburgites; Sp-Lhz: spinel-lherzolites; Pl-Lhz: plagioclase-lherzolites).

Sam ple	Nat ure	SiO 2	Ti O ₂	Al ₂ O ₃	Cr ₂ O ₃	Fe O	M gO	M nO	Ni O	Zn O	Ca O	SU M	C r#	M g#	Fe ₃ #
<i>Massif du Sud</i>															
25- 1A chr2	Hz	0.0 3	0.0 2	14. 72	50. 89	24. 39	9.7 3	0.1 3	0.0 7	0.2 2	< D .L.	100. 20	0. 70	0. 47	0.0 7
25- 1A chr4	Hz	0.0 3	0.0 2	13. 21	51. 60	24. 52	9.6 0	0.1 6	0.0 8	0.2 3	0.0 1	99.4 7	0. 72	0. 48	0.0 8
15- 1B chr2	Hz	0.0 2	< D .L.	17. 92	50. 72	18. 85	11. 67	0.1 6	0.0 3	0.0 3	0.0 2	99.4 2	0. 66	0. 56	0.0 2
15- 1B chr3	Hz	0.0 2	0.0 2	17. 58	50. 35	19. 90	11. 08	0.1 3	0.0 2	0.1 7	< D .L.	99.2 7	0. 66	0. 53	0.0 3
<i>Koniambo massif</i>															
xx31 42 chr1	Hz	< D .L.	0.0 1	22. 08	47. 61	16. 47	11. 81	0.3 2	0.0 8	0.2 3	< D .L.	98.9 5	0. 59	0. 56	< 0. 01
xx31 41 chr3	Hz	< D .L.	0.0 3	23. 80	47. 23	13. 60	14. 07	0.2 5	0.0 7	0.1 7	< D .L.	99.5 5	0. 57	0. 65	< 0. 01
xx31 34 chr2	Hz	< D .L.	0.0 1	27. 65	42. 11	15. 36	13. 52	0.2 5	0.0 7	0.1 3	< D .L.	99.3 1	0. 51	0. 62	< 0. 01
xx31 24 chr1	Hz	< D .L.	0.0 2	15. 46	55. 62	15. 52	11. 87	0.3 1	0.0 6	0.1 8	< D .L.	99.3 7	0. 71	0. 58	< 0. 01
<i>Tiebaghi massif</i>															
8- 10I chr2	Sp- Lhz	0.0 2	0.0 3	40. 02	28. 06	15. 10	16. 08	0.1 1	0.2 0	0.1 1	0.0 1	99.7 4	0. 32	0. 69	0.0 2
8- 10I chr3	Sp- Lhz	0.0 3	0.0 3	38. 96	30. 32	13. 30	17. 18	0.0 8	0.1 8	0.1 8	0.0 1	100. 26	0. 34	0. 73	0.0 2
8- 10I	Sp- Lhz	0.0 2	0.0 2	39. 32	30. 00	14. 16	16. 91	0.0 2	0.1 9	0.1 2	0.0 1	100. 77	0. 34	0. 71	0.0 2

Sam ple	Nat ure	SiO 2	Ti O2	Al2 O3	Cr2 O3	Fe O	M gO	M nO	Ni O	Zn O	Ca O	SU M	C r#	M g#	Fe3 #
chr4															
8- 10I chr6	Sp- Lhz	0.0 3	0.0 3	38. 22	30. 71	13. 45	17. 08	0.0 9	0.2 3	0.0 3	0.0 2	99.9 0	0. 35	0. 73	0.0 2
<i>Poum massif</i>															
7- 1A chr7	Pl- Lhz	0.0 5	0.3 4	23. 56	41. 15	21. 94	12. 14	0.1 8	0.1 4	0.1 9	0.1 0	99.7 9	0. 54	0. 57	0.0 6
7- 1A chr9	Pl- Lhz	0.0 2	0.3 4	25. 35	40. 71	21. 26	13. 12	0.1 3	0.1 3	0.2 6	0.0 4	101. 35	0. 52	0. 60	0.0 6
Pou m 13	Pl- Lhz	0.0 2	<D .L.	43. 25	23. 47	14. 51	16. 98	0.1 7	<D .L.	<D .L.	<D .L.	98.6 8	0. 27	0. 72	0.0 2
Pou m 11	Pl- Lhz	0.0 1	<D .L.	27. 17	41. 29	17. 12	13. 50	0.3 0	<D .L.	<D .L.	<D .L.	99.5 3	0. 50	0. 62	0.0 2

Table 3. Measured clinopyroxene rare earth element concentrations. Values for the reference material BCR-2 are from Jochum and Nohl (2008).

Sample name	Ti 48-06	Ti 50	Ti 50	Ti 50	Ti 50	Poum 13	Poum 13	Poum 13	Poum 11	Poum 11	Poum 11	BCR-2	BCR-2
Cpx name	MA06a17	MA06a03	MA06a04	MA06a05	MA06a07	MA06a35	MA06a36	MA06a38	MA06a41	MA06a42	MA06a43	Standard	Reference
Ce	0.008	0.028	0.006	0.006	0.029	0.047	0.050	0.034	0.022	0.013	0.038	52.8	53.3
Pr	0.011	0.015	0.002	< D.L.	0.014	0.009	0.011	0.016	0.006	0.007	0.010	6.69	6.70
Nd	< D.L.	0.176	0.326	< D.L.	0.074	0.108	0.134	0.131	0.072	0.039	0.111	27.3	28.9
Sm	0.142	0.130	0.162	0.166	0.152	0.160	0.305	0.159	< D.L.	0.019	0.030	6.62	6.59
Eu	0.071	0.093	0.099	0.099	0.105	0.094	0.066	0.072	0.016	0.012	0.011	1.94	1.97
Gd	0.493	0.507	0.645	0.616	0.684	0.488	0.596	0.463	0.102	0.117	0.116	6.71	6.71
Tb	0.135	0.145	0.167	0.165	0.186	0.146	0.156	0.136	0.031	0.028	0.026	1.00	1.02
Dy	1.06	1.22	1.33	1.28	1.31	1.21	1.23	1.19	0.35	0.28	0.28	6.70	6.44
Ho	0.263	0.286	0.332	0.322	0.355	0.293	0.327	0.272	0.105	0.087	0.075	1.32	1.27
Er	0.849	0.922	1.06	1.06	1.05	0.993	1.05	0.992	0.339	0.355	0.275	3.69	3.70
Tm	0.126	0.143	0.169	0.165	0.159	< D.L.	0.530	0.510					
Yb	0.854	0.880	1.04	1.08	1.06	0.996	1.14	0.985	0.480	0.352	0.388	3.62	3.39
Lu	0.130	0.125	0.152	0.140	0.144	0.159	0.154	0.152	0.065	0.058	0.056	0.530	0.500

Table 4. References and parameters used for the dry and hydrous melting models.

	Dry melting	Hydrous melting
<i>References</i>		
Equations	Incremental non modal batch melting (Shaw, 1970)	Dynamic melting ([Langmuir et al., 1977] and [Shaw, 2000])
<i>Model parameters</i>		
Source	Spinel lherzolite	
REE composition	McDonough and Sun, 1995 (enriched mantle source) Niu and Hékinian, 1997 (depleted mantle source)	Calculated from the Dry melting model
Partition coefficients	Niu and Hékinian, 1997	
<i>Initial mineralogy</i>		
Olivine	58%	68%
Orthopyroxene	19%	20%
Clinopyroxene	18%	7%
Spinel	5%	5%